

**INVESTIGATION OF HALOTAG FUSION PROTEIN FUNCTION  
IN *E. COLI* AND *PLASMODIUM***

**MD. GOLAM RIZVEE AHMED**

**A THESIS SUBMITTED IN PARTIAL FULFILLMENT  
OF THE REQUIREMENTS FOR THE DEGREE OF  
MASTER OF SCIENCE (BIOCHEMISTRY)  
FACULTY OF GRADUATE STUDIES  
MAHIDOL UNIVERSITY  
2014**

**COPYRIGHT OF MAHIDOL UNIVERSITY**

Thesis  
entitled  
**INVESTIGATION OF HALOTAG FUSION PROTEIN FUNCTION  
IN *E. COLI* AND *PLASMODIUM***

.....  
Mr. Md. Golam Rizvee Ahmed  
Candidate

.....  
Asst. Prof. Thanat Chookajorn,  
Ph.D. (Biochemistry, Molecular and Cell  
Biology)  
Major advisor

.....  
Lect. Ornachuma Itsathiphaisarn,  
Ph.D. (Molecular Biophysics and  
Biochemistry)  
Co-advisor

.....  
Mr. Philip James Shaw  
Ph.D. (Genetics)  
Co-advisor

.....  
Prof. Banchong Mahaisavariya,  
M.D., Dip Thai Board of Orthopedics  
Dean  
Faculty of Graduate Studies  
Mahidol University

.....  
Asst. Prof. Kittisak Yokthongwattana,  
Ph.D. (Agricultural and Environmental  
Chemistry)  
Program Director  
Master of Science Program in  
Biochemistry  
Faculty of Science, Mahidol University

Thesis  
entitled  
**INVESTIGATION OF HALOTAG FUSION PROTEIN FUNCTION  
IN *E. COLI* AND *PLASMODIUM***

was submitted to the Faculty of Graduate Studies, Mahidol University  
for the degree of Master of Science (Biochemistry)

on  
September 17, 2014

.....  
Mr. Md. Golam Rizvee Ahmed  
Candidate

.....  
Prof. Sakol Panyim, Ph.D. (Biochemistry)  
Chair

.....  
Asst. Prof. Thanat Chookajorn, Ph.D.  
(Biochemistry, Molecular and Cell  
Biology)  
Member

.....  
Lect. Ornchuma Itsathiphaisarn, Ph.D.  
(Molecular Biophysics and Biochemistry)  
Member

.....  
Mr. Philip James Shaw, Ph.D.  
(Genetics)  
Member

.....  
Lect. Sittiporn Pattaradilokrat, Ph.D.  
(Molecular Genetics)  
Member

.....  
Prof. Banchong Mahaisavariya,  
M.D., Dip Thai Board of Orthopedics  
Dean  
Faculty of Graduate Studies  
Mahidol University

.....  
Prof. Skorn Mongkolsuk, Ph.D.  
(Biological Science)  
Dean  
Faculty of Science  
Mahidol University

## ACKNOWLEDGEMENTS

First of all, I would wish to express my deep appreciation to all of them who gave me the possibility to accomplish this M.Sc. thesis. I am profoundly indebted to my advisor Asst. Prof. Thanat Chookajorn, for his time, guidance, important suggestions and technical support in his laboratory throughout my research and grateful for staying aside during my financial burden throughout my M.Sc studies. A Special thank goes to Dr. Philip James Shaw, my co-advisor for his passion, deliberate encouragement and enough freedom of doing experiments, providing useful advices, most importantly for available fund to accomplish my research work in his laboratory in Protein-Ligand Engineering and Molecular Biology Laboratory at BIOTEC, NSTDA. I also thank to Prof. Yongyuth Yuthavong for his suggestions and comments at the end of my thesis work. I am also very grateful to Dr. Ornachuma Itsathiphaisarn for becoming one of my thesis committee member.

I also express my deep appreciation to Pongpisid Koonyosying for his cooperation towards accomplishment of *P. berghei* transfection and flow cytometry data (unpublished work) at BIOTEC. I am also thankful to Dr. Chairat Uthaipibull for his assistance towards the fluorescence microscopy experiment (unpublished work) at BIOTEC. I appreciated to Mrs. Parichat Prommana for *P. falciparum* transfection work at BIOTEC. I also appreciated to Dr. Warangkhan Songsungthorng for her kind gift of *PbANKA*-EGFP parasite strain. I also highly appreciated to Ms. Nattida for her kind of DKO *E. Coli* cell line. I would like to appreciate to Dr. Prachumporn Nounrai for her assistance and support for operating confocal microscope at BIOTEC. I am thankful to Dr. Pattanop Kanokratana (Bioassay laboratory, BIOTEC) for his kind gift of pZero2 plasmid. I deeply appreciated to Dr. Tavi K. Neklesa and Dr. Craig Martin Crews (Yale University, USA) for their kind gift of HaloTag2 plasmid and HyT hydrophobic ligands. I also want to thank to Dr. Plearnpis Luxananil (Food Technology Laboratory, BIOTEC) for her kind gift of pLPPR3 plasmid. I am also thankful to Dr. Lingyu Guan for his kind gift of pBADEviB plasmid. I am grateful to BIOTEC and staff for their excellent technical support. I also thank to the team of Protein-Ligand Engineering Laboratory for their cooperation and discussions with various time points of my experiment. At last, I would like to thank our Department of Biochemistry for generous scholarship support for study and thesis. Also grateful to the Faculty of Science, Mahidol University for teaching assistantship and scholarship support throughout my study years that gives me an opportunity to pursue this M.Sc. degree.

Md. Golam Rizvee Ahmed

# INVESTIGATION OF HALOTAG FUSION PROTEIN FUNCTION IN *E. COLI* AND *PLASMODIUM*

MD. GOLAM RIZVEE AHMED 5436036 SCBC/M

M.Sc. (BIOCHEMISTRY)

THESIS ADVISORY COMMITTEE: THANAT CHOOKAJORN, Ph.D.,  
ORNCHUMA ITSATHIPHAISARN, Ph.D., PHILIP JAMES SHAW, Ph.D.

## ABSTRACT

HaloTag (HT) is a modified bacterial haloalkane dehalogenase enzyme that has been developed as a multi-purpose tool for studying protein functions, including protein purification, intracellular protein localization, time-dependent labeling, and control of intracellular protein levels. Ligand-mediated control of intracellular protein is an attractive tool for drug target validation. The function of HT was initially tested in *E. coli*. EGFP-HT fusion protein was functional when expressed in *E. coli*, although the expression was markedly lower than expected. Another reporter protein, dihydrofolate reductase thymidylate synthase (DHFR-TS) was used as a fusion partner to HT and its function was tested in *E. coli*. It was observed that the fusion of HT to DHFR-TS protein lowered the expression and intracellular activity of DHFR-TS compared with a 6x His tagged DHFR-TS. The DHFR-TS-HT fusions had correspondingly lower DHFR activity to complement a DHFR-TS *E. coli* mutant. The expression of the EGFP-HT fusion protein was also tested in the blood stages of the *Plasmodium berghei* rodent malaria parasite. Correct integrants were validated by PCR. EGFP-HT mRNA expression was detected by RT-PCR in transgenic EGFP-HT parasite lines. However, no EGFP-HT fusion protein was detected by Western blot. In conclusion, HT can be expressed as a fusion protein, but the low levels of protein activity suggest that HT interferes with fusion protein expression and/or stability in *E. coli* and *Plasmodium sp.*

KEY WORDS: HALOTAG / REVERSE TRANSCRIPTION PCR (RT-PCR) /  
PROTEIN EXPRESSION/ FUSION PROTEIN

71 pages

## CONTENTS

	<b>Page</b>
<b>ACKNOWLEDGEMENTS</b>	<b>iii</b>
<b>ABSTRACT</b>	<b>iv</b>
<b>LIST OF TABLES</b>	<b>x</b>
<b>LIST OF FIGURES</b>	<b>xi</b>
<b>LIST OF ABBREVIATIONS</b>	<b>xii</b>
<b>CHAPTER I      INTRODUCTION</b>	<b>1</b>
1.1 Genetic tools used to study <i>Plasmodium sp</i>	1
1.2 Reverse genetic tools for knockdown of target expression	2
1.2.1 RNAi and RNaseP mediated knockdown of gene expression	2
1.2.2 TET-Off regulation	4
1.2.3 <i>glmS</i> ribozyme mediated knockdown	5
1.3. Modulating the expression of gene at post-translational level	6
1.3.1 N-end rule and degron based tuning of the target gene expression	6
1.3.2 Cellular quality control mechanisms	7
1.3.3 Development of HaloTag for protein studies	8
<b>CHAPTER II      AIMS AND OBJECTIVES</b>	<b>13</b>
<b>CHAPTER III     MATERIALS AND METHODS</b>	<b>15</b>
3.1 Materials for molecular biology	15
3.1.1 Enzymes	15
3.1.2 Oligonucleotides	15
3.1.3 Kits	15
3.1.4 Plasmids	16
3.2 Techniques used in molecular biology	18
3.2.1 <i>E. coli</i> competent cell preparation	18
3.2.2 Bacterial transformation using heat shock method	18

## CONTENTS (cont.)

	Page
3.2.3 Agarose gel electrophoresis	19
3.2.4 Protein concentration analysis by Bradford assay	19
3.2.5 Molecular cloning	19
3.2.6 Construction of pET17b-EGFP-HT2 <sup>D106A</sup> by site-directed mutagenesis	20
3.2.7 Circular polymerase extension cloning of pBAD- CcdB-HT2 and pBAD-CcdB-HT7 constructs	21
3.3 Functional analysis of GFP-HaloTag protein function in bacteria	22
3.3.1 Expression and solubility analysis of EGFP-HT <sup>WT</sup> and EGFP-HT <sup>D106A</sup> fusion protein	22
3.3.2 Fusion protein analysis by Western blot	23
3.3.3 EGFP-HT fusion protein labeling by TMR	23
3.3.4 Fluorometric assay for the EGFP signal from EGFP-HT fusion protein	24
3.3.5 Determination the effect of HyT13 hydrophobic ligand on the stability of EGFP-HT fusion protein	24
3.3.6 Western blot detection of EGFP-HT:HyT complexes	24
3.4 Characterization of DHFRTS-HT protein function in <i>E. coli</i>	25
3.4.1 DHFR-TS activity assay in <i>E. coli</i>	25
3.4.1.1 Protein expression and activity assay of DHFR	25
3.4.1.2 TMR labeling of bacterial DHFRTS-HT fusion protein	25
3.4.1.3 Functional complementation test in bacteria expressing DHFRTS-HT	25

## CONTENTS (cont.)

	Page
3.5 Characterization of CcdB-HT toxic fusion protein function in <i>E. coli</i>	26
3.5.1 Characterize the activity of CcdB-HT2 and CcdB-HT7 fusion protein using TMR labeling	26
3.6 Functional analysis of HaloTag protein in <i>Plasmodium</i>	26
3.6.1 Characterization of HaloTag in <i>Plasmodium falciparum</i> parasite	26
3.6.1.1 Genomic DNA extraction and PCR detection of <i>P. falciparum</i> transgenic line	26
3.7 Characterization of HaloTag in <i>Plasmodium berghei</i> parasite	27
3.7.1 Mature schizonts isolation, plasmid transfection and genotyping of <i>P.berghei</i>	27
3.7.1.1 Parasites transfection and drug selection	27
3.7.1.2 Analysis of EGFP-HT gene expression in <i>P. berghei</i>	27
3.7.1.3 Protein isolation from transgenic parasite and Western blot	28
<b>CHAPTER IV      RESULTS</b>	<b>30</b>
4.1 Functional Analysis of GFP-HT protein in <i>E. coli</i>	30
4.1.1 Generation of bacterial expression vector carrying GFP-HT <sup>WT</sup> and GFP-HT <sup>D106A</sup>	30
4.1.2 EGFP-HT2 protein expression, Western blot detection and fluorophore labeling	32
4.1.3 Fluorometric assay and effect of hydrophobic ligands on EGFP-HT fusion protein stability	33
4.2 Analysis of DHFRTS-HT fusion protein activity in <i>E. coli</i>	37



## CONTENTS (cont.)

	<b>Page</b>
4.2.1 Recombinant plasmid construction, heterologous expression of DHFRTS-HT fusion protein and DHFR activity analysis	38
4.2.2 Detection of TMR labeled full-length DHFRTS-HT protein	39
4.2.3 Functional complementation among the bacterial strains	40
4.3 Activity of HaloTag on toxic protein	42
4.3.1 plasmid construction and TMR labeling of full-length CcdB-HT fusion protein	43
4.3.2 Bacterial strain expressing CcdB-HT fusion protein	44
4.4 HaloTag utilities in <i>Plasmodium</i>	45
4.4.1 Transgenic plasmid construction which contains <i>Pf</i> DHFRTS-HT fusion protein coding region	46
4.4.2 Confirmation of positive transfectant in <i>Plasmodium</i> <i>falciparum</i>	46
4.5 HaloTag expression in <i>P. berghei</i> parasite	47
4.5.1 Generation of transgenic parasites expressing EGFP-HT fusion protein	48
4.5.2 Confirmation of transgenic DNA integration in transfectants	48
4.5.3 Expression of transgenic EGFP-HT at the RNA level	50
4.5.4 Western analysis of EGFP expression in transgenic parasites	50
<b>CHAPTER V      DISCUSSION</b>	<b>52</b>
5.1 EGFP-HT2 function in <i>E. coli</i>	52
5.2 DHFRTS-HT2 and DHFRTS-HT7 function in <i>E. coli</i>	53

**CONTENTS (cont.)**

	<b>Page</b>
5.3 CcdB-HT2 and CcdB-HT7 function in <i>E. coli</i>	54
5.4 HT7 function in <i>P. falciparum</i>	55
5.5 Fusion protein interference by HT7 for other proteins	56
5.6 EGFP-HT2 function in <i>P. berghei</i>	57
5.7 HT2 as a tool for controlling protein levels in <i>Plasmodium</i>	58
<b>CHAPTER VI      CONCLUSION</b>	<b>60</b>
<b>REFERENCES</b>	<b>61</b>
<b>BIOGRAPHY</b>	<b>71</b>

## LIST OF TABLES

<b>Table</b>		<b>Page</b>
1.1	Summary of RNAi studies in <i>Plasmodium</i> species	3
3.1	Oligonucleotide primers used in this research	17
3.2	Recipe for SDS-PAGE	18
5.1	UPR homologous proteins in <i>P. falciparum</i> (Pf) and <i>P. berghei</i> (Pb)	59

## LIST OF FIGURES

Figure	Page
1.1 Schematic catalytic diagram of wild type and mutant dehalogenase (DhaA) activity	10
1.2 Schematic diagram of HaloTag mediated protein degradation strategy	12
4.1 Plasmid maps of pET17b carrying HaloTag <sup>WT</sup> and HaloTag <sup>D106A</sup> mutant fragment	31
4.2 Detection of EGFP-HT fusion protein by Western blot and fluorophore labeling	33
4.3 Fluorometric assay for measuring the activity of EGFP-HT <sup>WT</sup> and EGFP-HT <sup>D106A</sup> fusion protein	36
4.4 Western blot of EGFP-HT fusion protein coupled with HyT13 ligand	37
4.5 Comparison of enzyme specific activity among bacterial strains	39
4.6 TMR labeling of full-length DHFRTS-HT7 and DHFRTS-HT2 protein	40
4.7 Complementation tests among the <i>E. coli</i> strain expressing DHFRTS enzyme	41
4.8 Detection of TMR labeled CcdB-HT fusion protein	44
4.9 Growth curve of <i>E. coli</i> expressing CcdB-HT fusion protein	45
4.10 Identification of <i>P. falciparum</i> transgenic parasite carrying <i>Pf</i> DHFRTS-HT7 episomal transfection vector	47
4.11 Construction of <i>Pb</i> EGFP-HT parasites	49
4.12 Detection of HaloTag transcript by Reverse Transcription PCR (RT-PCR)	50
4.13 Parasite protein transferred into PVDF membrane	51

## LIST OF ABBREVIATIONS

A	Absorbance
Asn	Asparagine
Asp	Aspartate
Amp	Ampicillin
ATc	Anhydrotetracycline
ALAS	aminolevulinate synthase 1
Bis-Tris	2-[Bis-2-hydroxyethyl)-amino]-2-hydroxymethyl-propane-1,3 diol
BSA	Bovine serum albumin
BiP	Binding immunoglobulin protein
CPP	Cell penetrating peptide
CcdB	Control of cell death in bacteria
CaCl <sub>2</sub>	Calcium chloride
CPEC	Circular polymerase extension cloning
CRM1	Chromosomal Maintenance 1
°C	Degree Celsius
CB2	Cannabinoid receptor protein 2
CHIP	C-terminus of Hsp70-interacting protein
dsRNA	double stranded RNA
DHF	7,8-Dihydrofolate (H <sub>2</sub> Folate)
DHFRTS	Dihydrofolate reductase thymidilate synthase
dNTP	Deoxy nucleotide triphosphate
dTMP	Deoxy thymidine monophosphate
dUMP	Deoxy uridine monophosphate
DTT	Dithiothreitol
DD	Degradation determinant
DKO	Double knockout
DAPI	4', 6-diamidino-2-phenylindole
eef-1 $\alpha$	Eukaryotic elongation factor 1 alpha

**LIST OF ABBREVIATIONS (cont.)**

EGS	External guiding sequence
EDTA	Ethylenediamine tetraacetic acid
EGFP	Enhanced green fluorescent protein
ERAD	Endoplasmic reticulum associated protein degradation
ER	Endoplasmic reticulum
FKBP12	Human FK506/rapamycin binding protein
GlcN6P	Glucosamine-6-phosphate activated ribozyme
Glu	Glutamine
Gly	Glycine
GS	Glutathione synthase
HRP	Horse reddish peroxide
HEK293	Human embryonic kidney 293
HSP70	Heat shock protein 70
HALTS	HaloTag stabilizer
HT	HaloTag
His	Histidine
HyT	Hydrophobic tag
HSP 86	Heat shock protein 86
HT2	HaloTag2
HT7	HaloTag7
HF	High fidelity
Ile	Isoleucine
IPTG	Isopropyl thiogalactoside
kV	Kilovolt
KCl	Potassium chloride
kDa	Kilodalton
KOAc	Potassium acetate
LB	Luria Bertani

## LIST OF ABBREVIATIONS (cont.)

Leu	Leucine
mRNA	messenger RNA
ml	Millilitre
mm	Millimetre
mM	Millimolar
μmol	Micromolar
μF	Microfarad
MalE	Maltose-binding protein
MgCl <sub>2</sub>	Magnesium chloride
μl	Microlitre
NaCl	Sodium chloride
ng	Nanogram
nM	Nanomolar
OD	Optical density
PfgyrA	<i>Plasmodium falciparum</i> gyrase A
PCR	Polymerase chain reaction
PAGE	Polyacrylamide gel electrophoresis
Pf	<i>Plasmodium falciparum</i>
PYR	Pyrimethamine
Phe	Phenylalanine
PBS	Phosphate buffer saline
Pb	<i>Plasmodium berghei</i>
PVDF	Polyvinylidene difluoride
RISC	RNA-induced silencing complex
RNAi	RNA interference
RT-PCR	Reverse transcription polymerase chain reaction
RFU	Relative fluorescent intensity
rpm	Revolutions per minute
siRNA	short interfering RNA

**LIST OF ABBREVIATIONS (cont.)**

SDS	Sodium dodecyl sulfate
Ser	Serine
ssu-rna	Small subunit of ribosomal RNA
THF	5,6,7,8-Tetrahydrofolate
TEMED	Tetramethylethylenediamine
TBST	Tris-Buffered Saline and Tween 20
tg	<i>Toxoplasma gondii</i>
Tris	2-Amino-2-hydroxymethyl-propane-1,3-diol
TetR	Tetracycline repressor
TetO	Tet operator
Thr	Threonine
Trp	Tryptophan
TMP	Trimethoprim
TMR	Tetramethyl rhodamine
Ub	Ubiquitin
UPR	Unfolded protein response
UV	Ultraviolet
WT	Wild



## CHAPTER I

### INTRODUCTION

#### 1.1 Genetic tools used to study *Plasmodium* sp.

Annually, millions of people are infected with the malaria parasite *Plasmodium falciparum* regarded as a deadly human parasite. Now a day, increasing resistance of human malaria parasite and mosquito vector against currently marketed drugs and insecticidal is making the malaria treatment less effective (1). Therefore, it is important to identify novel and effective antimalarials for targeting every stage of the parasite lifecycle for complete elimination of parasites, including those that are resistant to current drugs (2). Most importantly, understanding of *Plasmodium* genomes is a prerequisite for discovery of new drugs against new genomic targets. In *Plasmodium* biology, major limitation of identifying novel drug targets is lack of reliable reverse genetic tools. Obviously, knowledge of essential *Plasmodium* genes is very important for design of novel and effective anti-malarial drugs, which can only be accomplished by functional studies of candidate genes. Despite the knowledge obtained from parasite genomes (3, 4) and genomic studies of RNA expression profiles (5, 6), our knowledge of gene function is far from complete. In the current version (11.1) of the *Plasmodium* species genomic information database, PlasmoDB (7), more than one-third (1766) of *P. falciparum* genes are annotated as “conserved *Plasmodium* protein, unknown function”, and so elucidation of their functions requires direct testing using genetic tools. Classical forward genetics is defined by the experiment in which an organism with a distinct phenotypic trait, or a mutant, is identified and gene(s) that are responsible are identified from analysis of heritable segregation patterns. Forward genetics has been applied in *Plasmodium*; for example, the primary genetic marker for the chloroquine resistant phenotype was mapped to a region of chromosome 7 (8). The causal mutation in the *Pfcr* gene in this region was confirmed by an allelic exchange forward-genetic approach (9). Recently in

*Plasmodium*, a forward genetic approach was developed using the transposable element *PiggyBac*, which originated from a *Lepidoteran*. In this approach, the *PiggyBac* element can insert randomly via TTAA homing sequences present all over the genome. *PiggyBac* insertions can disrupt gene expression and thus give rise to mutant parasites. After selection of parasites with the phenotype of interest, the gene responsible can be identified by PCR walking from the *PiggyBac* insertion site (10, 11). In spite of efficient integration of *PiggyBac* in *Plasmodium*, this system is not practical for saturation mutagenesis of every gene in the genome since isolating clones is laborious, and disruption of genes important for blood stage growth is not possible. This is because *Plasmodium* maintains a haploid state during the blood stages.

In this regard, reverse genetic tools are necessary for validating essential genes expressed in asexual stages of *Plasmodium* parasite. Gene knockout is the classical reverse genetic strategy to determine gene function from null mutant phenotype, in which the target gene is perturbed by homologous recombination, and the genetically modified parasite can be selected and characterized (12). Creating a knockout parasite is only possible for non-essential genes owing to the haploid nature of *Plasmodium* blood-stages cultured in the laboratory. If repeated attempts at knockout are unsuccessful, the target is assumed to be essential, although it is difficult to rule out technical/experimental design problems. However, there is no mutant phenotype that can be observed to determine precisely the function of such essential genes. Although, genetic knockout is not practical for studying the function of essential *Plasmodium* genes, attenuating their expression is an excellent alternative experimental strategy to generate a mutant loss-of-function phenotype for providing insight into gene function. Attenuation can be performed at both the post-transcriptional and the post-translational level.

## **1.2 Reverse genetic tools for knockdown of target expression**

### **1.2.1 RNAi and RNaseP mediated knockdown of gene expression**

Across diverse eukaryotic organisms, RNA interference (RNAi) can naturally modulate the expression of genes at post-transcriptional stage. RNAi is

widely used as an orthodox reverse-genetic technique for knockdown of specific target genes, including those that are essential for survival and development. The RNAi process is started by recognition of dsRNA by Dicer and Drosha which is a RNase III endonuclease enzymes followed by the processing of dsRNA into 20-25 nucleotide short interfering RNAs (siRNAs) (13) which is further loaded to the RNA-induced silencing complex (RISC) and helicase-unwound in a sequence specific manner to produce single-stranded siRNA. The single stranded siRNA binds to target mRNA, leading to degradation or inhibition of mRNA translation mediated by RNaseH enzyme Argonaute. To attenuate gene expression in a particular cell type, introducing a sequence specific siRNA directly into cells, or expressing a short-hairpin RNA from a transgene can get around the first stage of dsRNA processing. There are several published reports describing attempts at RNAi to silence genes in the blood stages of *Plasmodium* parasite. In these reports, attenuation of gene expression was mediated by long dsRNA introduced by electroporation into *P. falciparum* infected red blood cells (14, 15), and adding high concentration of siRNA into culture medium (16, 17), or by siRNA injection into mice that were infected with *P. berghei* (18). In these studies, down-regulation of the target gene leading to significant parasite growth defects was observed, suggesting that an RNAi like pathway might exist in malaria parasites (Table 1.1).

**Table 1.1: Summary of RNAi studies in *Plasmodium* species**

Author	Experimental design	% Knockdown	Observed phenotype	Control experiment
Kumar <i>et al.</i> , 2002(Pf)	dsRNA(282 nM)	70	Altered parasite growth after 24 hr	Luciferase siRNA
McRobert <i>et al.</i> , 2002(Pf)	dsRNA(94 nM)	60	Altered parasite growth after 72 hr	water
Mohammed <i>et al.</i> , 2003(Pb)	siRNA(1.87µM)	40-50	Altered parasite growth after 56 hr	GFP siRNA
Dasaradhi <i>et al.</i> , 2005(Pf)	siRNA(7.5µM)	60-70	Altered parasite growth after 56 hr	Untreated parasite
Tuteja <i>et al.</i> , 2008(Pf)	dsRNA(3.75µM)	55	Altered parasite growth after 48 hr	GFP siRNA

Average molecular weight of 19-mer siRNA or dsRNA sequence is approximately 13300 g/mol

Pf = *Plasmodium falciparum* ; Pb = *Plasmodium berghei*

Despite these claims of RNAi though, all the aforementioned studies used high concentration of dsRNA or siRNA (more than 1  $\mu$ M ; typically <100 nM is used), and the maximum level of attenuation achieved was low compared with other species with canonical RNAi pathways (>90% knockdown of target gene is typical in a mammalian cell line). A later study to formally test for RNAi using rigorous bioinformatics search concluded that *Plasmodium* lacks Dicer and Argonaute, and thus lacks a canonical RNAi pathway. Moreover, transgenic parasites were generated expressing short-hairpin RNA and no significant reduction of target gene expression was observed (19). Therefore, the phenotypes generated in other studies perhaps not the results of targeting a specific gene but could be a non-specific effect caused by excess siRNA or dsRNA in *Plasmodium*. Alternatively, the knockdown and resulting phenotypes might be a weaker antisense effect whereby the annealing of antisense transcript to its target mRNA inhibits mRNA translation. Although, antisense transcripts are exists in *P. falciparum* transcriptome but functional roles are yet to be elucidated (20). Recently, a novel knockdown strategy employing ribonuclease P (RNaseP) ribozyme in *E. coli* was demonstrated in *P. falciparum* for characterizing *PfgyrA* essential gyrase gene function (Augagneur *et al.*, 2012). In *E. coli*, ribonuclease P is regarded as a type of hammerhead ribozyme that is guided by external guiding sequence (EGS) RNA that binds to its complementary target mRNA and cleaves the target efficiently (22). An external morpholino oligonucleotide was designed as an analogue of EGS to bind to *PfgyrA* mRNA, which was covalently linked with cell penetrating peptide (CPP). The morpholino inhibited *PfgyrA* mRNA expression up to 60% and led to growth inhibition. However, this strategy may not be widely applicable because synthesizing the external morpholino sequence is expensive and is a rather complicated task in the lab. Moreover, the *in vivo* off-target activity and general applicability of this approach is unknown.

### 1.2.2 TET-Off regulation

Alternative methods have been developed to attenuate gene expression in malaria parasite at the level of transcription using a TET transactivator, which was first established in the related apicomplexan parasite *Toxoplasma gondii* (23). In mammalian cell, Tet-Off system was developed to control the target gene expression.

Tet-Off system was required 2 components such as tetracycline repressor (TetR) protein and VP16 transcriptional activator protein that derived from *Herpes simplex* virus. Tet-Off system was simply constructed by the fusion of TetR with the VP16 protein. The fusion of TetR with VP16 converted TetR into an efficient transactivator (tTA) controlled by small molecule tetracycline, or its derivatives such as anhydrotetracycline (ATc). A minimal promoter sequence fused with binding sites for TetR (Tet operator, TetO) is required for transcription initiation by the transactivator (24). Mechanistically, the transactivator binds to TetO to initiate transcription of the transgene. The affinity between TetR and TetO is therefore reduced by the addition of tetracycline or ATc and turned off the gene transcription. This system is thus known as the “Tet-Off” system for controlling gene expression (24, 25). To apply the Tet-Off system for reverse genetics in *T. gondii*, two sequential integrations are needed; at first, to integrate a Tet-Off regulated complementing gene copy in un-specified location of the genome via non-specific integration, and double crossover homologous recombination was required for knockout the endogenous copy of the gene. The expression of the complementing gene copy regulated under TetO promoter can be knocked-down upon the addition of ATc to the parasite culture medium. This Tet-Off system appears to be functional for controlling episomal reporters in *P. falciparum* (26) but it is impractical for reverse genetics because double homologous integration is very rare in *P. falciparum* (27). Recently, an improved Tet-Off system has been developed in *P. berghei* (28); however, this may still be technically challenging to use in *P. falciparum* as it requires integration of large DNA construct by double homologous recombination in 5' gene flanking regions.

### 1.2.3 *glmS* ribozyme mediated knockdown

Another method has recently been developed using the *glmS* ribozyme for post-transcriptional control of the target gene in *P. falciparum* (30). The *glmS* ribozyme is a short RNA sequence conserved in gram-positive bacteria that has also been demonstrated to control reporter gene expression in yeast *Saccharomyces cerevisiae* (29). Catalytically, the *glmS* ribozyme requires the small molecule cofactor glucosamine-6-phosphate (GlcN6P) for self-cleavage. Therefore, the cofactor can be applied exogenously to activate cleavage and lead to mRNA degradation in an

experimentally controlled fashion. The utility of *glmS* ribozyme has successfully reported in *P. falciparum* for controlling the activity of GFP and essential *PfDHFR*-TS protein, and the essential PlasmepsinV protein (31). This knockdown strategy is impractical in *P. berghei* *in vivo* mouse model because of the rapid excretion of glucosamine sugar by the animal, which limits knockdown efficiency (G. Akinola & P. Shaw, unpublished data, personal communication).

### 1.3. Modulating gene expression at the post-translational level

#### 1.3.1 N-end rule and degron based tuning of target gene expression

To control the expression of any gene at its protein levels requires developing new tools in which take advantage of cellular protein quality control machineries. Naturally, unstable amino acid residues at the N-terminus of any protein is depicted its *in vivo* stability which so called “N-end rule” (32). As a consequence of this rule, a short-lived protein termed a degron or destabilizing domain (DD) can destabilize target protein in eukaryotes when it fused to the N-terminus part (33). The DD engages a cascade of cellular proteolysis pathways for degradation of target protein. The cellular proteolysis cascade is started by activation of ubiquitin (Ub) via E1 enzyme. Then, Ub is transferred to E2 Ub-conjugating enzymes that sequentially transfer Ub to E3-Ub ligase. Finally, Ub is tagged to lysine residues of the respective protein substrate, which triggers ATP-dependent degradation of substrate, by the 26S proteasome (34). Different DDs have been developed, and the rate of protein degradation for some can be controlled by small molecule ligands, which bind specifically to the DD. Shield-1 ligand was first demonstrated to regulate protein abundance in mammalian cells in which Shield-1 ligand stabilizes the ddFKBP degron and any protein fused to it. In contrast, when ligand is absent, fusion protein is degraded (35). Two DD systems such as FKBP12-Shield-1 and *E. coli* DHFR DD has recently developed to control the expression of target gene in *P. falciparum*. In these systems, the target gene is altered by integration of DD encoding DNA sequence. The DD fusion can be stabilized by specific ligands such as Shield-1 (FKBP12-Shield system) or trimethoprim (ecDHFR system). These DD-based systems have been used

to demonstrate the functions of some essential *P. falciparum* genes (37, 38, 39). However, the current DD tools are not generally applicable since many proteins are not destabilized efficiently, or the insertion of DD is not tolerated when fused to N-terminal part of the target protein (40). Perhaps of the N-end rule (41), some DD fusion protein has no destabilizing effect in the absence of respective ligand required for its stabilization. Hence, a C-terminal degron may have little impact on fusion protein stability if the N-terminal portion (protein of interest) is very stable. To date, all applications of DD systems for knockdown of endogenous essential proteins have utilized when DD fused at the C-terminus. DD fused to the N-terminal is not practical since it would require integration of transgenic DNA by double homologous crossover, which is very inefficient in *P. falciparum*. Moreover, many drug targets such as enzymes are constitutively expressed at high levels and are unlikely to be efficiently deregulated using this system, since the published work has been demonstrated for proteins expressed at low levels and/or in a stage specific manner.

Moreover, the stabilizing ligands must be added continuously to parasite cultures prior to the knockdown experiment. This limitation is a major barrier, since the Shield-1 and trimethoprim ligands are bioactive, and the parasite can adapt and become resistant to their controlling effects (39). To overcome the problem of continuous supply of stabilizing ligands, the FKBP12-Shield1 system has very recently been modified to work in the opposite manner in transiently transfected mammalian cells, i.e. ligand induced-degradation (41). This alternation has no impact of the problem governing by N-end rule pathway of fusion protein stability. Moreover, the preparation of Shield-1 is synthetically challenging and very expensive for animal studies.

### **1.3.2 Cellular quality control mechanisms**

Combining synthetic cell permeable small molecules and utilizing cellular quality control would be an advantage to knockdown any protein of interest *in vivo*. In principle, protein folding is dependent upon entropy change in which ordered water molecules are excluded as hydrophobic protein residues internalize (42). Therefore, when hydrophobic residues are exposed to solvent, this is recognized in the cell as unfolded protein, which is then tagged by ubiquitin and followed by targeting the

protein for degradation in proteasome (42, 43). Degrading any unfolded protein by proteasome is the result of generating the unfolded protein response (UPR). During the translation of mRNA, folding process of the secreted nascent polypeptide chain is started in the cytoplasm, which is processed further in the endoplasmic reticulum (ER) to their respective cellular destination via secretory pathways for proper function (44).

Protein folding is assisted by different class of existing molecular chaperones and factors in the cells and protein activities are also critically monitored in a coordinated fashion. Protein intermediates, or those which failed to maintain their native form, or incorrectly folded protein intermediates are sent to the ER for quality control surveillance and by the ER assisted degradation (ERAD) pathway, which destroys the unfolded or aberrantly folded protein (45). In the ERAD processing sites, there are several conserved folding factors such as BiP, disulfide isomerase and other specific factors that are necessary for recognition and targeting to the misfolded protein (46). Thus, accumulation of incorrectly folded protein in the cytosol activates the UPR pathways followed by employing molecular chaperone to destroy the unfolded protein through the ubiquitin-proteasome system (UPS) (43, 47). Recently, a system has been developed for controlling target protein abundance *in vivo* using a HaloTag system which engages the cellular UPR mechanism for control of target protein level (48). This system is described in more detail below.

### **1.3.3 Development of HaloTag for protein studies**

HaloTag is an engineered protein tag developed by rational protein engineering of bacterial encoded haloalkane dehalogenase (DhaA) derived from *Rhodococcus rhodochrous* (49). The DhaA enzyme acts to detoxify various haloalkane compounds by converting them into acid and alcohol products (49). Owing to the broad substrate specificity of dehalogenase catalysis, *Rhodococcus* bacteria have been applied for bioremediation of oil-polluted water into alcohol and acid. The 34kDa DhaA enzyme contains a catalytic triad in its active site that cleaves the carbon-halogen bond of aliphatic halogenated (haloalkane) compounds by a hydrolysis mechanism. In the wild-type dehalogenase enzyme, the catalysis reaction is started by the cleavage reaction of a carbon-halogen bond that occurs upon binding the haloalkane compound to the active site of dehalogenase enzyme. A transient covalent



complex is formed between enzyme and haloalkane substrate. Thereafter, terminal halogen is removed by Asp106 and further produces alcohol and acid as a catalytic byproduct. (49). The broad substrate specificity of DhaA is attractive for development as a biotechnological tool, since many different haloalkane ligands with different properties can interact with DhaA. The Promega Corporation developed variants of DhaA that can form stable covalent complexes with different haloalkane ligands (50, 51, 52). Activation of water molecules involving His273 of DhaA is required for hydrolysis of the transient covalent complex. To modify the DhaA enzyme, the protein-ligand intermediate is stable when His273 is replaced with Phe, which has no general base to carry out the hydrolysis reaction. Therefore, the covalently linked haloalkane substrate remains trapped in the active site of the mutant enzyme. Further mutations were made to improve ligand association kinetics so that covalent complexes with the mutant can form rapidly. The final mutant dehalogenase was then initially marketed as a fusion tag protein named HaloTag2 (HT2) (**Figure 1A**). HT2 has a major drawback as a fusion protein in that it has low intracellular solubility in both cell free system and *E. coli*, which affects the level of expression and function of its fusion partner (53). A more structurally stable version of HT2 named HaloTag7 (HT7) was developed by random mutagenesis of HT2. HT7 contains a sequence of Ser-Thr-Leu-Glu-Ile-Ser-Gly at the C-terminus (291-297), which was found provide structural stability, and also function better as a fusion protein at both the N- and C-terminal positions (53). The mutations in HT7 also increased the accessibility of the respective haloalkane ligand for irreversible attachment to the dehalogenase active site, leading to improved association binding kinetics. Thereafter, Promega marketed HT7 to replace HT2, which was later discontinued. The use of HT7 as a tool for protein studies is dependent on the haloalkane ligand's properties, such as fluorescent labels and affinity handles. Therefore, in mammalian and *E. coli* host, HaloTag can be applied as a tool for a variety of protein applications including expression, purification of recombinant protein, localization of proteins in situ and proteomics (50, 52, 54). These broad applications are made possible because a wide variety of haloalkane compounds can form a covalent complex with HaloTag protein.

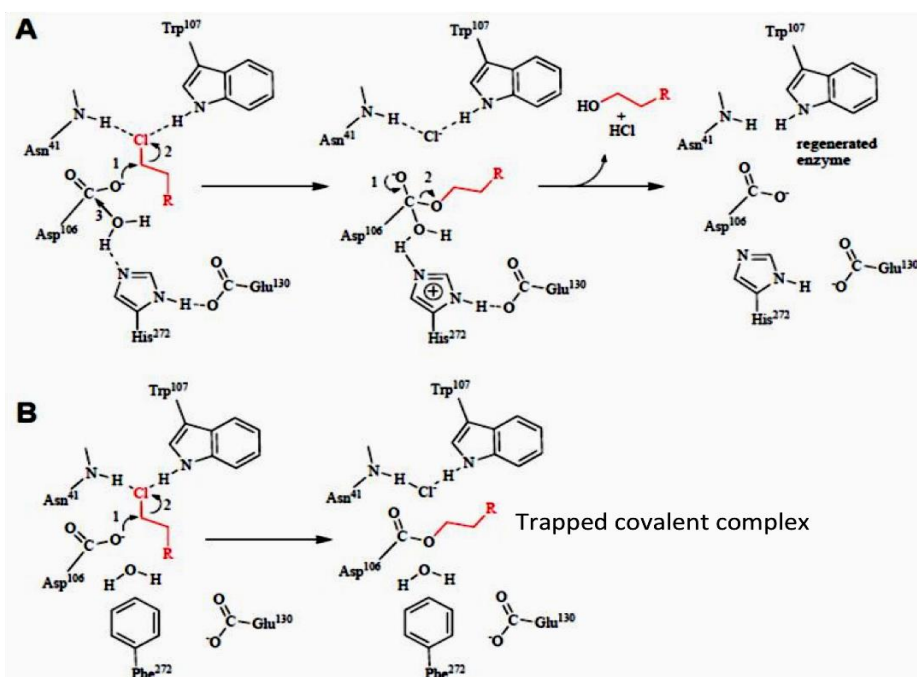


**Figure 1.1: Schematic catalytic diagram of wild type and mutant dehalogenase (DhaA) activity.** (A) In the catalytic triad of wild type DhaA, nucleophile Asp 106 attacks the  $\alpha$ -carbon of the chloroalkane to form a transient covalently bonded alkyl-enzyme intermediate and displacing the Cl as a leaving group, which is stabilized by Asn41 and Trp107. His272 act as a general base releasing the products by hydrolysis from the active site and enzyme prepares for next round of catalysis. (B) To trap the covalent intermediate, His272 replaced with Phe that cannot act as a general base and is unable to hydrolyze the alkyl-enzyme intermediate and chloroalkane ligand is irreversibly bound with Asp106 residue. (49).

Recently, one application of HT2 has been reported in which it can be used to control target protein abundance by selectively engaging the cellular quality control machineries in mammalian cells and whole animals (48). In this work, proteins of interest were fused to HT2, and the fusion proteins can form highly specific, rapid and covalent complexes with synthetic ligands containing chloroalkane-reactive linker via the HT2 domain. Various hydrophobic ligands with chloroalkane reactive linkers were synthesized and tested. It was found that a novel compound called HyT13, which

carries a stable, hydrophobic and highly cell permeable adamantyl moiety, was able to activate efficient *in vivo* degradation of HT2-fused protein. Degradation of HaloTag-fused protein when complexed with HyT13 ligand was also shown to be proteasome-dependent as expected (49). The utilization of UPR is the key strategy for applying HaloTag as a post-translational reverse genetics tool. The hydrophobic moiety of HyT13 compound induces the degradation of HaloTag fusion protein because HT:HyT13 complex is recognized as an unfolded protein, or in other words, the hydrophobic moiety of HyT13 mimics unfolded protein. The HT:HyT13 complex associates with the molecular chaperone heat shock protein 70 (HSP70) and E3 ubiquitin ligase for targeted protein destruction (55).

The HT:HyT13 DD system for controlling protein stability as described by Neklesa *et al.* 2011 at one level operates in an opposite manner to the FKBP12/Shield-1 and *E. coli* DHFR protein DD systems since the targeted protein is degraded upon addition of hydrophobic tagged chloroalkane ligand. Without any ligand, protein is otherwise stable. The HT:HyT13 DD system has several advantages over the other tools described above. Most importantly, N- or C-terminal expression of HT exerts its function efficiently as a fusion protein. In various cell types, the HyT13 compound is not bioactive (48), unlike TMP and Shield1. In *Plasmodium*, HaloTag has been utilized for studying localization of a *Plasmodium falciparum* gametocyte protein (56), but it has never been applied in *P. berghei*. Currently available tools to characterize the function of essential genes are limited for *Plasmodium*, and no tool exists for controlling gene expression post-transcriptionally in *P. berghei*. Thus, the HT:HyT13 system could be a useful tool for elucidating essential gene function in *Plasmodium* and for validating potential drug targets.

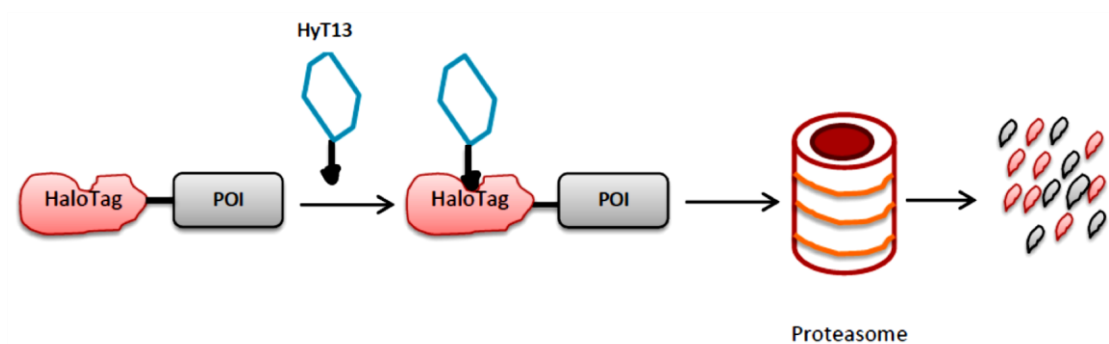


**Figure 1.2: Schematic diagram of HaloTag mediated protein degradation strategy.** Hydrophobic part of the haloalkane ligand is surface exposed upon binding with HaloTag fusion protein. This hydrophobic complex is recognized as unfolded protein and targeted to the proteasome for further destruction.

## **CHAPTER II**

### **AIMS AND OBJECTIVES**

#### **Aims:**

1. Functional characterization of HaloTag fusion proteins in *E. coli* bacteria.
2. Functional characterization of HaloTag as a fusion protein in the *P. berghei* and *P. falciparum* blood stage parasite.

#### **Objectives:**

##### **A. In bacterial expression system**

- A.1. To perform site-directed mutagenesis to make mutant HT2 control gene having mutation D106A.
- A.2. To construct a bacterial recombinant plasmid containing EGFP-HT2<sup>WT</sup> and EGFP-HT2<sup>D106A</sup> mutant.
- A.3. To perform the recombinant protein expression and extraction from *E. coli* BL21 strain.
- A.4. To perform fluorescence labeling using TMR ligand and Western blot using anti-GFP primary antibody to detect the activity EGFP-HT fusion protein.
- A.5. To measure the EGFP activity using spectrofluorometer and effect of the HyT13 upon binding to HaloTag.
- A.6. To construct recombinant vectors containing DHFR<sup>TS</sup>-HT2 and DHFR<sup>TS</sup>-HT7 fusion gene.
- A.7. To perform specific activity of DHFR using enzyme assay, bacterial complementation and TMR labeling.

A.8. To clone the HT2 and HT7 fusion at the C-terminus of *E. coli* toxic CcdB protein.

A.9. To characterize the activity of CcdB-HT fusion using TMR labeling and bacterial growth assay.

## **B. In *Plasmodium* model**

### **B.1. In *P. falciparum* host**

B.1.1 To construct transgenic plasmid containing C-terminus of HT2 and HT7 gene fused to DHFRTS protein.

B.1.2 To generate transgenic lines of parasites expressing C-terminus DHFRTS-HT2 and DHFRTS-HT7 protein.

B.1.3 To perform genotyping by PCR.

B.1.4 To perform TMR labeling in the transgenic parasite and study the localization of DHFRTS-HT fusion protein via confocal microscope.

### **B.2. In *P. berghei* host**

B.2.1 To construct transfection plasmid DNA containing EGFP-HT2<sup>WT</sup> and EGFP-HT<sup>D106A</sup> protein coding sequence.

B.2.2 To generate stable transgenic lines of *P. berghei* parasites *in vivo* with single transgene integrations expressing EGFP-HT2<sup>WT</sup> and EGFP-HT2<sup>D106A</sup> fusion protein.

B.2.3 To perform genotyping by PCR, reverse transcriptionPCR (RT-PCR).

B.2.4 To extract EGFP-HT2 protein from *P. berghei* and detect by Western blot.

## CHAPTER III

### MATERIALS AND METHODS

#### 3.1 Materials for molecular biology

##### 3.1.1 Enzymes

Restriction endonucleases *NotI* (GC<sup>∇</sup>GGCCGC), *HindIII* (A<sup>∇</sup>AGCTT), *EcoRV* (GAT<sup>∇</sup>ATC), *XbaI* (T<sup>∇</sup>CTAGA), *BamHI* (G<sup>∇</sup>GATCC), *DpnI* (G<sup>m</sup>6A<sup>∇</sup>TC), *PstI* (CTGCA<sup>∇</sup>G), *KpnI* (GGTAC<sup>∇</sup>C), *NcoI* (C<sup>∇</sup>CATGG), *ApaI* (GGGCC<sup>∇</sup>C), *SacII* (CCGC<sup>∇</sup>GG) and T4 DNA ligase, T4 DNA polymerase, and antarctic phosphatase. All above-mentioned enzymes were purchased from New England Biolabs (NEB, USA)

##### 3.1.2 Oligonucleotides

All oligonucleotides listed in table 3.1 were synthesized by following vendors: Integrated DNA Technologies (IDT), Singapore through Thailand distributor (Ward Medic Ltd.), 1<sup>st</sup> Base (Malaysia) and Biodesign (Thailand).

##### 3.1.3 Kits

GeneMark Plasmid Miniprep Kit (GMBiolab Co. Ltd., Taiwan), E.Z.N.A. Gel and PCR Clean Up Kit (Omega Biotek, USA) and Geneaid Genomic DNA Extraction Kit (Geneaid Biotech. Ltd., Taiwan) were used for plasmid DNA extraction, PCR product purification, gel extraction, and genomic DNA isolation from parasite, respectively.

### 3.1.4 Plasmids

Plasmid pCDNA5/FRT/EGFPHaloTag2 (provided by Dr. Taavi Neklesa and Professor Craig M. Crews, Yale University, USA) contains EGFP-HT2 fusion gene fragment.

Plasmid pZero2 (Invitrogen) contains CcdB toxic protein coding sequence. This plasmid was a kind gift from Dr. Pattanop Kanokratana (Bioassay laboratory, BIOTEC).

Plasmid pET17b (Novagen, Germany) used as a bacterial expression vector. It contains the Ampicillin (Amp<sup>®</sup>) resistance gene and multiple cloning sites for the insertion of target gene. It also contains an inducible T7 promoter that controls the expression of target protein.

Plasmid pBAD33 (ATCC, USA) used as a bacterial expression vector. It contains the chloramphenicol (Cam<sup>®</sup>) resistance gene and multiple cloning sites for the insertion of target gene. It contains araC promoter and rrnBT1, rrnBT2 terminator regulatory elements for regulating the expression of the target gene using arabinose as an inducer.

Plasmid pLPPR3 (57) contains natural GFP protein (protein I.D. AAC53663.1) expressed under a strong constitutive promoter L-lactate dehydrogenase (*pldhL*) of *L. sakei*. This plasmid also carrying Erythromycin resistant cassette for plasmid selection

Plasmid pL0017 was used as a *Plasmodium* expression vector (58). This plasmid possesses several important elements such as *pb-eef-1α*, a constitutive promoter that drives high expression of target gene, a non-essential *d-ssu-rrna* sequence is present in this vector which is homologous to *P. berghei* genome for targeted integration (59), and the presence of *tgdhfr-ts* marker is used for selecting transgenic parasites resistant to pyrimethamine drug.

Hydrophobic chloroalkane ligands HyT13 and HyT36 were also provided by Dr. Taavi Neklesa and Professor Craig M. Crews (Yale University, USA). Both of these ligands carry the same adamantane hydrophobic moiety, but differ in the length of haloalkane linker part.



**Table 3.1: Oligonucleotide primers used in this research**

Name	Sequences (5'-3') □	Base (nt)	T <sub>m</sub> ** (°C)	Restricti-on site
HT2-Fp	AAAAGGTACCTCCGAAATCGGTACAGGCTTCC	32	68	<i>KpnI</i>
HT2-Rp	AAAAGTGCAGTTAGCCGGCCAGCCCGG	27	71	<i>PstI</i>
GS-Fp	CTACTGAAGCTTCGTTTGCTTTACAAATCGATC	33	59	<i>HindIII</i>
GS-Rp	CTACTGGGGCCCAGATAAAGGGTTCATTTTGTTC	36	58	<i>ApaI</i>
ALAS-Fp	TACTGGGGCCCATGTCCCATAGGAAAAGCCA	31	61	<i>ApaI</i>
ALAS-Rp	CTACTGCCGCGGTGGTGAAGCACCTATACATG	32	56	<i>SacII</i>
Pf-TS-Fp	AAGGTACCAGCAGCCATATCCATTGAAATTTTTCA	36	69	<i>KpnI</i>
DHFR3-UTR-Rp	AAGGTACCGTTCAGGTAATTTTGTGCATC	28	52	<i>KpnI</i>
DHFR-BamHI-Fp	AAGGATCCATGATGGAACAAGTCTGCGACGTTTC	35	71	<i>BamHI</i>
HaloTag-R-PstI	AAAAGTGCAGTTAACCGGAAATCTCCAGAGTAGACA	36	65	<i>PstI</i>
SD-UNIp	ATCCTCTAGAGTCGACCTGCAGAGGAGGAATTCACCATG	39	61	<i>XbaI</i>
pBAD-UNIp	CCGCCAAAACAGCCAAGCTT	20	68	<i>HindIII</i>
HT2-DA-Fp	GTCATCCACGcCTGGGGCTC	20	71	-
HT2-DA-Rp	GAGCCCCAGGcGTGGATGAC	20	71	-
5'-ssuFp (P1)	TGTTGGGTTATCAAATACCATCAAAAATGA	30	67	-
5'-ssuRp (P3)	TACCGCACAGATGCGTAAGGAGAA	24	68	-
3'-ssuFp (P2)	GTTGAAAAATTAAAAAAAAC	21	50	-
3'-ssuRp (P4)	CTAAGGTACGCATATCATGG	20	55	-
Linker-CcdB-Fp	AGGAGGAATTCACCATGCAGTTTAAGGTTTACACCTATAAA	42	53	-
Linker-CcdB-Rp	GGATGAGTTTGTATCTCGAGCTATTCCCCAGAACATCAGGTT	32	60	-
Linker-HT2-Fp	GCTCGAGATACAAACTCATCC	21	58	-
HT2-pBAD-Rp	CCGCCAAAACAGCCAAGCTTCGCCACTGTGCTGGATATCTTA	42	64	-
Linker-HT7-Fp	GCTCGAGATACAAACTCATCCGGATCCGAATCGGTACTG	40	59	-

□ Underlining represents the restriction recognition site

\*\*Melting temperature was calculated using NEB T<sub>m</sub> calculator.

**Table 3.2: Recipe for SDS-PAGE**

	12% separating gel	4% stacking gel
0.5 M Tris HCl, pH 8.8	1.25 ml	-
1.5 M Tris HCl, pH6.8	-	0.50 ml
40% Acrylamide	1.5 ml	0.2 ml
10% SDS	50 $\mu$ l	20 $\mu$ l
30% Ammonium persulfate	25 $\mu$ l	10 $\mu$ l
TEMED	2.5 $\mu$ l	2 $\mu$ l
Water	2.18 ml	1.272 ml
Total	5.0075 ml per gel	2.004 ml per gel

## 3.2 Techniques used in molecular biology

### 3.2.1 *E. coli* competent cell preparation

In every step, bacterial cells were collected by low-speed centrifugation at  $4,000 \times g$  at  $4^\circ\text{C}$ . Overnight bacterial inoculum was diluted at 1:100 into 200 ml of LB broth and continuously cultured at  $37^\circ\text{C}$ , 200 rpm for 2-3 hours until  $A_{600}$  reaching 0.4-0.5. Cells were then immediately put on ice for 15 min. After that, cell pellet was collected by low-speed centrifugation. 20 ml of 0.1 M ice-cold  $\text{MgCl}_2$  was used to resuspend. Cell pellet was recollected by low-speed centrifugation. The pellet was washed with 20 ml pre-chilled 0.1 M  $\text{CaCl}_2$  and further incubated on ice for 1 hour. Thus, cell pallet was harvested by low-speed centrifugation and resuspended with 4 ml of ice-cold  $\text{CaCl}_2$ , 50% glycerol and stored at  $-80^\circ\text{C}$  freezer.

### 3.2.2 Bacterial transformation using heat shock method

Frozen *E. coli* competent cell was mixed gently with plasmid DNA and incubated on ice for 30 min. Heat shock transformation was performed at  $42^\circ\text{C}$  for 1 min and then quickly transferred the tube back on ice. After 3 min, 700  $\mu$ l of LB broth

was mixed with the suspension. Transformed cells were cultured at 37 °C for 1 hour and plated on LB agar with appropriate drug selection.

### 3.2.3 Agarose gel electrophoresis

0.8% of agarose (SeaKem, USA) was prepared in 0.5X TAE electrophoresis buffer. DNA sample premixed with 6X loading dye (NEB) was loaded into well. Electrophoresis was performed at 100 volt for 30 min and subsequently stained with ethidium bromide for 20 min. DNA migration was visualized by UV transillumination (300-365 nm).

### 3.2.4 Protein concentration analysis by Bradford assay

Bradford colorimetric assay was used to determine protein concentration (90). A standard dilution of purified bovine serum albumin (BSA) was prepared to calculate the total protein concentration of unknown protein sample. BSA concentration was determined and calculated using  $A_{279} = 44.680 \text{ M}^{-1}\text{cm}^{-1}$ . BSA was diluted from 2–16 µg and added into 1 ml of Bradford reagent (GE Healthcare, USA) with 10 min incubation at room temperature. The signal was measured by  $A_{595 \text{ nm}}$  absorbance

### 3.2.5 Molecular cloning

The vectors were constructed by PCR cloning or sub-cloning. The detail is as follows. EGFP-HT<sup>WT</sup> fragment was obtained from pCDNA/FRT/EGFPHaloTag2 plasmid. Bacterial T7 promoter-based vector pET17b-DHFRTS-k1 was replaced by DHFRTS-HT7 and DHFRTS-HT2. DHFRTS-HT7 was PCR amplified from the pDHFRTS-HT7 vector using of Dhfrts-HT7-Fp and Dhfrts-HT7-Rp primer pair. HT2 fragment was also PCR amplified from pCDNA5/FRT/EGFPHaloTag2 plasmid using HT2-Fp and HT2-Rp primers. PCR condition for DHFRTS-H7 insert was as follows: 30 cycles of 10 s at 94 °C, 20 s at 55 °C and 3 minutes at 72 °C. For HT2 amplification, PCR condition was as follows: 30 cycles of 20 s at 98 °C, 5 s at 98 °C, 15 s at 60 °C and 20 s at 72 °C. For malarial transfection with pDHFRTS-GFP-HT7-glms vectors, pGEM-HT7 and pDHFRTS-GFP-glms plasmids were digested with *KpnI/PstI* under recommended conditions. For the construction of pDHFRTS-GFP-

HT2-glms, the HT2 gene fragment was PCR amplified from pCDNA5/FRT/EGFP-HaloTag2 using HT2-Fp and HT2-Rp primers (**Table 3.1**). PCR conditions were started at initial denaturation 20 s at 98 °C, 10 s denaturation step at 98 °C, 15 s annealing at 60 °C annealing and 20 s extension at 72 °C and 5 minutes for last extension step at 72 °C. For the Construction of pL0017-EGFP-HT<sup>WT</sup> and pL0017-EGFP-HT<sup>D106A</sup> parasite expression vectors, EGFP-HT<sup>WT</sup> and EGFP-HT<sup>D106A</sup> genes were sub-cloned from pET17b plasmid into parasite expression vector pL0017. 15 µg of pET17 plasmid DNA carrying EGFP-HT<sup>WT</sup> and EGFP-HT<sup>D106A</sup> open reading frame were digested with *HindIII* and *EcoRV*-HF in 1X NEB buffer 2 at 37 °C for 2 hour. The restriction enzyme conditions for PCR cloning were based on recommended protocols from the companies. The enzyme for each primer was listed in **Table 3.1**. DNA fragments were prepared by gel purification by commercial purification kit. 1:3 ratio of vector and insert was used for ligation in 10 µl of total reaction volume at 12 °C for approximately 20 hours. Using the heat shock transformation method, approximately half of the ligation reaction was transformed into *E. coli* DH5α competent cell and selected with appropriate antibiotics. Several colonies from the transformed bacterial plates were cultured at 37 °C for 16 hours. DNA plasmid was extracted using GeneMark Plasmid Miniprep Kit. Integrity and orientation of insert was tested by restriction enzyme digestion and DNA sequencing.

### 3.2.6 Construction of pET17b-EGFP-HT2<sup>D106A</sup> by site-directed mutagenesis

pET17b-EGFP-HT<sup>WT</sup> plasmid was used to change the aspartate residue at 106 position to alanine in HaloTag wild type sequence. Mutagenic primers (**Table 3.1**) were design by following the protocol described on the QuickChange site directed mutagenesis site (Stratagene). Mutagenesis reactions were performed using forward and reverse primers separately as suggested by Wang *et al.*, 1999. 80 ng of pET17b-EGFP-HT<sup>WT</sup> plasmid DNA was used in the mutagenesis reaction. 50 µl of reaction contains 0.5 µM of mutagenic primer, 200 µM dNTP, 1X HF buffer, 3 mM of MgCl<sub>2</sub> and HF-Phusion DNA polymerase (2 units). Thermal cycler was set up as follows: 98 °C for 30 s, 15 cycles of 98 °C for 10s, 72 °C for 5 min with additional 72 °C for 5 min in the final step. Half of the reaction was mixed with 3 units of HF-Phusion DNA

polymerase. Mutagenesis reaction was repeated for 15 cycles with previously described cycling conditions following by digestion with 4 unit of *DpnI* enzyme for eliminating original plasmid template at 37 °C for 4 hour. After that, 0.8% agarose gel electrophoresis was performed to confirm *DpnI* digested plasmid. DNA was transformed in to *E. coli* and confirmed by DNA sequencing.

### **3.2.7 Circular polymerase extension cloning of pBAD-CcdB-HT2 and pBAD-CcdB-HT7 constructs**

Circular polymerase extension cloning (CPEC) method was used for cloning of each fragment into pBAD vector (90). Primers were designed to have an overlapping region at the end of the sequences where vector and insert was hybridized and extended until reaching the 5' end for successful completion of full circle. PCR primers were designed for CcdB and HT gene amplification with the overlapping region at the 5' end. 10 ng of plasmid template and 10µM of primers were used. Linker-CcdB-Fp and linker-CcdB-Rp primers were used for amplifying CcdB from pZero2 plasmid (Invitrogen). Linker-HT2-Fp and HT2-pBAD-Rp primers were used to amplify HT2 from pCDNA5/FRT/EGFPHaloTag2. Linker-HT7-Fp and HT7-pBAD-Rp primers were used to amplify HT7 from pFC20A-HaloTag7-Flexi-SP6 (Promega). Vector templates were denatured at 98 °C for 10 s. Annealing temperature was varied depending on the target amplicon. For CcdB, HT2 and HT7 gene, annealing temperature was done at 56 °C, 61 °C and 59 °C for 20 s, respectively. Polymerase extension was performed at 72 °C for 1 min per kilobase for 25 cycles. PCR reaction mixture contains 200 µM of dNTPs, 1X HF-buffer, and 1 unit of Phusion polymerase enzyme. pBAD33 vector was linearized by restriction digestions with *XbaI/HindIII* enzymes at 37 °C for 2 hour. E.Z.N.A PCR purification kit was used for plasmid purification. Linearized vector and purified CcdB-HT PCR fragments were mixed together at equimolar ratio and performed another CPEC reaction. In this CPEC, pBAD-UNIp and SD-UNIp primer pairs were used due to having overlapping region with the 3' end of CcdB-HT fragment. 50 µl of Standard PCR was performed in following cycling conditions: denaturation of linear pBAD vector at 98 °C for 10 s, 25 cycles at 55 °C for 20 s and 72 °C for 2 min, extension step required at last at 72 °C for 5 min. Initially, full recombinant plasmid was analyzed by 0.8% agarose gel

electrophoresis to identify full-length 6.5 kb pBAD-CcdB-HT plasmid. *E. coli* XL-1 blue cell was transformed with 5 µl of CPEC reaction using heat shock and selected the positive clones on LB agar plate containing 34µg/ml chloramphenicol with 2% glucose. Transformed plates were incubated into 37 °C for overnight and 6 colonies were picked up from pBAD-CcdB-HT2 and pBAD-CcdB-HT7 plate. Plasmids were extracted using commercial kit and mapped with restriction analysis using *XbaI/HindIII* enzyme to validate the correct clones containing CcdB-HT fusion gene fragment. Thus, recombinant plasmids were also sequenced to determine the orientations and integrity of CcdB-HT fragment.

### 3.3 Functional analysis of EGFP-HT protein function in bacteria

#### 3.3.1 Expression and solubility analysis of EGFP-HT<sup>WT</sup> and EGFP-HT<sup>D106A</sup> fusion protein

*E. coli* BL21 (DE3) competent cell was prepared for heat shock transformation of pET17b recombinant plasmids carrying EGFP-HT<sup>WT</sup> and EGFP-HT<sup>D106A</sup> fusion protein coding sequence. One colony from each plate was inoculated into LB-ampicillin (100µg/ml ampicillin) broth and continuously cultured at 37 °C in 200 rpm incubator shaker for overnight. Therefore, inoculum was diluted to (1:100) new 10 ml LB-ampicillin broth and continuously cultured 37 °C in 200 rpm until A<sub>600</sub> reaching 0.5-0.6. Induction of both EGFP-HT<sup>WT</sup> and EGFP-HT<sup>D106A</sup> fusion protein was started by 1mM IPTG and continuously cultured for 16 hours. Induced bacterial cell collected at 12,000  $\times$  g for 10 min in 1 ml cold HaloTag buffer (150 mM NaCl, 50 mM HEPES, pH 7.5, 1 mM DTT and 0.5 mM EDTA) was used for sonication. Sonication was performed at 50% amplitude with VibraCell ultra sonicator (4 min total time; 10 s on / 20 s off). After sonication, cell mixture was centrifuged at 10,000  $\times$  g for 10 min at 4 °C. Yellowish supernatant was transferred into new ice-chilled 1.5 ml eppendorf tubes.

### **3.3.2 Fusion protein analysis by Western blot**

There are 10, 5 and 1  $\mu$ g dilutions of total protein were prepared from the stock protein solution contains EGFP-HT fusion protein. Diluted proteins were then mixed with protein loading dye and boiled at 95 °C for 10 min. SDS-PAGE was performed at 150 volt, 400 mA for 90 min. Protein bands in gel were transferred into a nitrocellulose membrane. In short, four pieces of filter paper were soaked with 1X transfer buffer. Excess SDS buffer was removed by soaking the gel in distilled water. Nitrocellulose membrane was placed between filter paper. Protein transfer tank was filled with 1X transfer buffer [25 mM Tris (Research organics, USA), 192 mM glycine (Research organics, USA) at pH 8.3]. Electrophoretic transfer was performed at 150 volt in 300 mA for 16 hours. After that, nitrocellulose membrane was soaked with Ponceau S stain solution approximately 10 min. Blocking step was performed using 5% skim milk diluted in TBST buffer (1X TBS at pH 8.0 and 0.05% tween 20) for 2 hours. Anti-GFP primary antibody diluted in TBST buffer (1:3000) was incubated with membrane at least for 2 hours at room temperature followed by subsequent washing 3 times with TBST buffer. Membrane was then incubated with anti-rabbit polyclonal HRP-secondary antibody (1:20,000 dilution) (Thermo Scientific) for 1 hour at room temperature followed by subsequent washing 3 times with TBST buffer. Chemiluminescence was used to detect specific signal of EGFP-HT fusion protein by exposing the treated membrane to X-ray film.

### **3.3.3 EGFP-HT fusion protein labeling by TMR**

Total protein was isolated from bacteria expressing EGFP-HT fusion protein and labeled with 1  $\mu$ M of HaloTag tetramethyl rodamine (TMR) ligand (Promega). Protein was mixed with SDS sample buffer at 95 °C for 10 min before being loaded into SDS gel. The gel was soaked with distilled water 3 times to remove excess SDS from the gel and scanned with a Typhoon 9410 scanner ( $E_{\text{ex}}$  = 532 nm;  $E_{\text{em}}$  = 580 nm).

### **3.3.4 Fluorometric assay for the EGFP signal from EGFP-HT fusion protein**

Activity of green fluorescent protein was detected with spectrofluorometer (FP-6500, Jasco, UK). Emission of EGFP was monitored at 395 nm excitation and 470/550 nm emission wavelengths. Initially, 100 µg of total protein was used for monitoring the fluorescent activity of EGFP protein. Crude extract of EGFP-HT fusion protein was mixed with 1 ml of pre-chilled 1X PBS and transferred to a 10 mm quartz cuvette and the EGFP signal observed at 509 nm with 200 nm/min scanning speed.

### **3.3.5 Determination the effect of HyT13 hydrophobic ligand on the stability of EGFP-HT fusion protein**

Protein extraction was performed according to the protocol in Section 3.3.1 with some modifications. 1X PBS was used for protein dilution instead of HaloTag buffer, and induction time was 4 hours after adding 1mM IPTG. Soluble protein extract from *E. coli* BL21 (DE3) with pET17b plasmid was used as a negative control. pLPPR3 plasmid expressing GFP<sub>uv</sub> protein isolated from the same BL21 (DE3) host was used as a positive control (57). 10 µg of total protein was used for testing the effect of HyT13 hydrophobic ligand. Stock solution of 100 µM of HyT13 ligand was prepared in ddH<sub>2</sub>O. HyT13 ligand was diluted to 10 µM in 1X PBS solution and mixed with 10 µg of total protein in 20 µl of final reaction volume following by incubation on ice for 60 min in order to allow covalent coupling of ligand with HaloTag protein. Ice-cold 1X PBS was added into the reaction to make 1 ml solution and transferred it into 10 mm quartz cuvette. Relative fluorescent intensity (RFU) was measured using spectrofluorometer (FP 6500, Jasco, UK). RFU was monitored at 395 nm excitation and 470/550 nm emission wavelengths. Scanning speed was at 200 nm/min with 4-second response time.

### **3.3.6 Western blot detection of EGFP-HT:HyT complexes**

HyT13 and HyT36 were prepared in ddH<sub>2</sub>O, and 10-fold dilution series ranging from 0.1 to 10 µM of ligand in 1XPBS was incubated with 10 µg of total protein with EGFP-HT for 60 min on ice. Samples were mixed with protein loading dye and denatured at 95 °C for 10 min. SDS-PAGE was performed. Protein was then



transferred overnight onto nitrocellulose membrane. The EGFP-HT target protein was detected by using a standard chemiluminescent method as described in section 3.3.2.

### **3.4 Characterization of DHFRTS-HT protein function in *E. coli***

#### **3.4.1 DHFR-TS activity assay in *E. coli***

##### **3.4.1.1 Protein expression and activity assay of DHFR**

DHFR activity assay was performed in 1 ml of DHFR buffer (1mg/ml of BSA; 100  $\mu$ M NADPH; 100  $\mu$ M DHF). At, DHFRTS-HT fusion protein activity was quantified by measuring the rate of NADPH consumption (340 nm absorbance) at room temperature. DHFR activity was determined based on the following equation:

$$\text{Activity} = [\Delta A_{340} / (123000 \times \text{volume of total protein})] \text{ mole/min/ml.}$$

##### **3.4.1.2 TMR labeling of bacterial DHFRTS-HT fusion protein**

10  $\mu$ g and 20  $\mu$ g of total protein were treated with 1  $\mu$ M of TMR fluorescent ligand for one hour on ice. SDS-PAGE was performed, and the result was analyzed by Typhoon imager at  $E_{\text{ex}}/E_{\text{em}} = 532/580$ .

##### **3.4.1.3 Functional complementation test in bacteria expressing DHFRTS-HT**

*E. coli* strain lacking *folA* and *thyA* was a gift from Ms. Nattida Suwanakitti (BIOTEC). pET17b-DHFRTS-HT vectors were transformed and plated on LB agar containing 100  $\mu$ g/ml ampicillin and 50 mg/ml thymidine. Colony from the LB plate was inoculated into new LB broth supplemented with thymidine and grown overnight at 37 °C. Overnight culture was diluted to 1:100 in new LB media until  $A_{600} = 0.05$ . Bacterial growth at 37 °C was measured every hour for eight hours based on  $A_{600}$  value.

### **3.5 Characterization of CcdB-HT toxic fusion protein function in *E. coli***

#### **3.5.1 Characterize the activity of CcdB-HT2 and CcdB-HT7 fusion protein using TMR labeling**

*E. coli* containing pBAD-CcdB-HT plasmid was cultured at 37 °C, 200 rpm incubator shaker overnight. Cultures were diluted to 1:100 into new 20 ml of LB broth with 34µg/ml chloramphenicol and cultured at 37 °C, 200 rpm until A<sub>600</sub> reached to 0.5-0.6 and 0.1% of L-arabinose was added into the culture and measure the A<sub>600</sub> until 8 hours. Therefore, 10 ml of bacteria culture were centrifuged at 10,000  $\times$  g, 4 °C for 20 min to collect bacterial cell pellet which then resuspended in HaloTag purification buffer and sonicated using Vibra-X ultrasonicator equipped with microtip at 50% amplitude (total 5 min; 10s on/20s off). Therefore, crude extract centrifugation at 4 °C, 10,000  $\times$  g for 10 min and transferred supernatant into new ice-chilled 1.5 ml centrifuge tubes. Concentration of total protein was measured by Bradford colorimetric assay. 15 µg of total protein was treated with 1µM of TMR ligand for 1 hour in ice. SDS-PAGE was performed and gel was scanned under typhoon scanner (GE healthcare, USA) at specific excitation and emission wavelength ( $E_{ex}/E_{em}$  = 532/580) and detected the TMR labeled CcdB-HT fusion protein.

### **3.6 Functional analysis of HaloTag protein in *Plasmodium***

#### **3.6.1 Characterization of HaloTag in *Plasmodium falciparum* parasite**

##### **3.6.1.1 Genomic DNA extraction and PCR detection of *P. falciparum* transgenic line**

Ms. Parichat Prommana performed all of the parasite transfection and malaria culture. *P. falciparum* 3D7 strain was cultured *in vitro* using the conditions described in Trager & Jensen *et al.*, 1976. Episomal PfDHFRTS-HT7 was extracted by using 0.02% Saponin and then resuspended in parasite lysis solution (1X PBS, 150 µg/ml proteinase K, 2% SDS). Phenol-chloroform–isoamyl alcohol

(25:24:1) solution was used for extraction of genomic DNA following by DNA precipitation with absolute ethanol and 0.3 M sodium acetate (97). Several primer pairs were used for PCR detection of episomal plasmid. Primer set 1 (Pf-TS-F<sub>P</sub>, DHFR3-UTR-R<sub>P</sub>) corresponded to the positive control that amplified bifunctional DHFR-TS gene at the PFD0830w locus. Primer set-2 (DHFR-BamHI-F<sub>P</sub>, HaloTag-PstI-R<sub>P</sub>) was used for amplification of 2.7 kb DHFTRTS-HT7 fusion gene sequence from transgenic parasites.

### **3.7 Characterization of HaloTag in *Plasmodium berghei* parasite**

#### **3.7.1 Mature schizonts isolation, plasmid transfection and genotyping of *P. berghei***

##### **3.7.1.1 Parasites transfection and drug selection**

Mr. Pongpisid Koonyosying performed all of the above parasite transfection, animal husbandry and *in vitro* culture and cloning. Parasite cells from Mr. Pongpisid Koonyosying were supplied for experiments as suspensions of infected red cells. *PbANKA* strain has been used as a reference strain for creation of isogenic parasite line expressing EGFP-HT fusion protein. Empty *PbANKA* was used as a negative control and another *PbANKA* parasite line was a gift from Dr. Warangkhan Songsunthorn at BIOTEC which is transfected with pL0017 plasmid (48) expressing EGFP protein regulated under the same *eef-1α* promoter and used as a positive control. Mature schizonts were collected from the *P. berghei* ANKA strain in order to perform parasite transfection with pL0017 plasmid carrying EGFP-HT<sup>WT</sup> and EGFP-HT<sup>D106A</sup> fusion protein coding sequence. Parasite transfection was performed based on Non-viral Nucleofactor technology described in Janse *et al.*, 2006.

##### **3.7.1.2 Analysis of EGFP-HT gene expression in *P. berghei***

Transgenic *P. berghei* expressing EGFP (*PbEGFP*), EGFP-HT<sup>WT</sup> (*PbEGFP-HT<sup>WT</sup>*), and EGFP-HT<sup>D106A</sup> (*PbEGFP-HT<sup>D106A</sup>*) parasites were obtained from mice after 10 days post-infection. *PbANKA* and *PbEGFP* parasite

strains were used as negative and positive controls, respectively. Parasites were saponin lysed and TriZol was used for total RNA extraction from parasites. Turbo DNase (Ambion) treatment was required for removal of trace amount of gDNA. Synthesizing cDNA was required 2 ug of total RNA treated with Superscript III reverse transcriptase (Invitrogen) using Oligo(dT<sub>21</sub>) primer. Reaction lacks reverse-transcriptase enzyme (-RT) was used as a control in parallel using the same quantities of RNA. cDNA samples were diluted 1:100 in deionized water and primers specific to HaloTag gene were used for reverse-transcription PCR. As an internal control, Glutathione Synthetase (GS) gene was used to amplify using specific primer. Standard PCR conditions are following: initial denaturation at 98 °C for 10 s, 30 cycles of amplification started with 10 s denaturation step at 98 °C, 20 s annealing step at 61 °C (50 °C for GS primer pair) and 60 s extension step at 72 °C and 5 minute for last extension step at 72 °C.

### **3.7.1.3 Protein isolation from transgenic parasite and Western blot**

Protein was isolated from transgenic *P. berghei* parasite lines expressing EGFP-HT<sup>WT</sup>, EGFP-HT<sup>D106A</sup> fusion protein. Therefore, total protein isolated from *PbANKA* and *PbEGFP* was used as negative and positive control respectively. Parasitemia was measured daily by Giemsa stain until it reached 20% and mice were sacrificed for collection of parasitized red blood cell following by centrifugation at 12,000  $\times$  g for 5 min and subsequently lysed the pellet with saponin for 3 min at room temperature to release parasites from red blood cell. After that, pellets were washed 3-4 times with 1X PBS to remove excess red blood cell from the suspension and stored at -80 °C overnight. Protein extraction buffer (1X PBS with 1X complete protease inhibitor (Roche)) was used to resuspend the parasite pellets. Protein extraction procedure was performed by using the freeze-thaw method in such that parasites were rapidly frozen by dipping the tubes into liquid-N<sub>2</sub> for 10 seconds and dipped into distilled water for 1-2 min to thaw them completely. This process was repeated for 4 times. The parasite pellet was performed by centrifugation at 4 °C in 13,000  $\times$  g for 10 min. Bradford assay was used for measuring protein concentration. Protein loading dye was added to 30  $\mu$ g of total protein and denatured for 10 min at 95

°C. Standard Western detection method was followed as described in previous section. Anti-HaloTag primary antibody (1:1000 dilution) was used to detect the EGFP fusion protein.

## CHAPTER IV

### RESULTS

#### 4.1 Functional Analysis of EGFP-HT protein in *E. coli*

Enhanced green fluorescent (EGFP) was previously used as a reporter protein controlled by the HaloTag DD together with HyT13 hydrophobic ligand (48). In this research, the same EGFP-HT2 fusion protein was tested in *E. coli*. Bacterial expression vector was constructed containing EGFP-HT2 fusion gene under T7 bacteriophage promoter. Western blot and TMR fluorophore labeling were performed to detect EGFP-HT2 fusion protein. Using fluorometry, the activity of EGFP-HT2 fusion was also measured, and the effect of HyT13 hydrophobic ligand on EGFP-HT2 activity was tested.

##### 4.1.1 Generation of bacterial expression vector carrying EGFP-HT<sup>WT</sup> and EGFP-HT<sup>D106A</sup>

The pET17b vector (Novagen) was used for cloning and expression of the EGFP-HT<sup>WT</sup> and EGFP-HT<sup>D106A</sup> proteins. The full length coding region (~1.6 kb) of EGFP-HT2 obtained from pCDNA5/FRT/EGFPHaloTag2 plasmid (a gift from Dr. T. Neklesa) was digested and cloned at the unique *NotI/HindIII* restriction sites of the pET17b vector. There is a flexible linker comprised of six amino acid residues (ARDTNS) in between EGFP and HT2 domains to ensure the proper folding and solubility upon translation. The pET17b plasmid contains the strong bacteriophage T7 promoter and terminator for efficient control of transcription of the target gene (**Figure 4.1A**). Wild-type HT2 protein can specifically form a covalent complex with haloalkane ligand, and a control plasmid was created to express a mutant HT protein that is unable to form covalent complexes with haloalkane ligands. From the literature, aspartate residue 106 of HT2 protein is critical for protein-ligand interaction, and mutation of this residue to alanine disrupts complex formation (48). Mutant HT2 was used as a negative control in this experiment (**Figure 4C**).

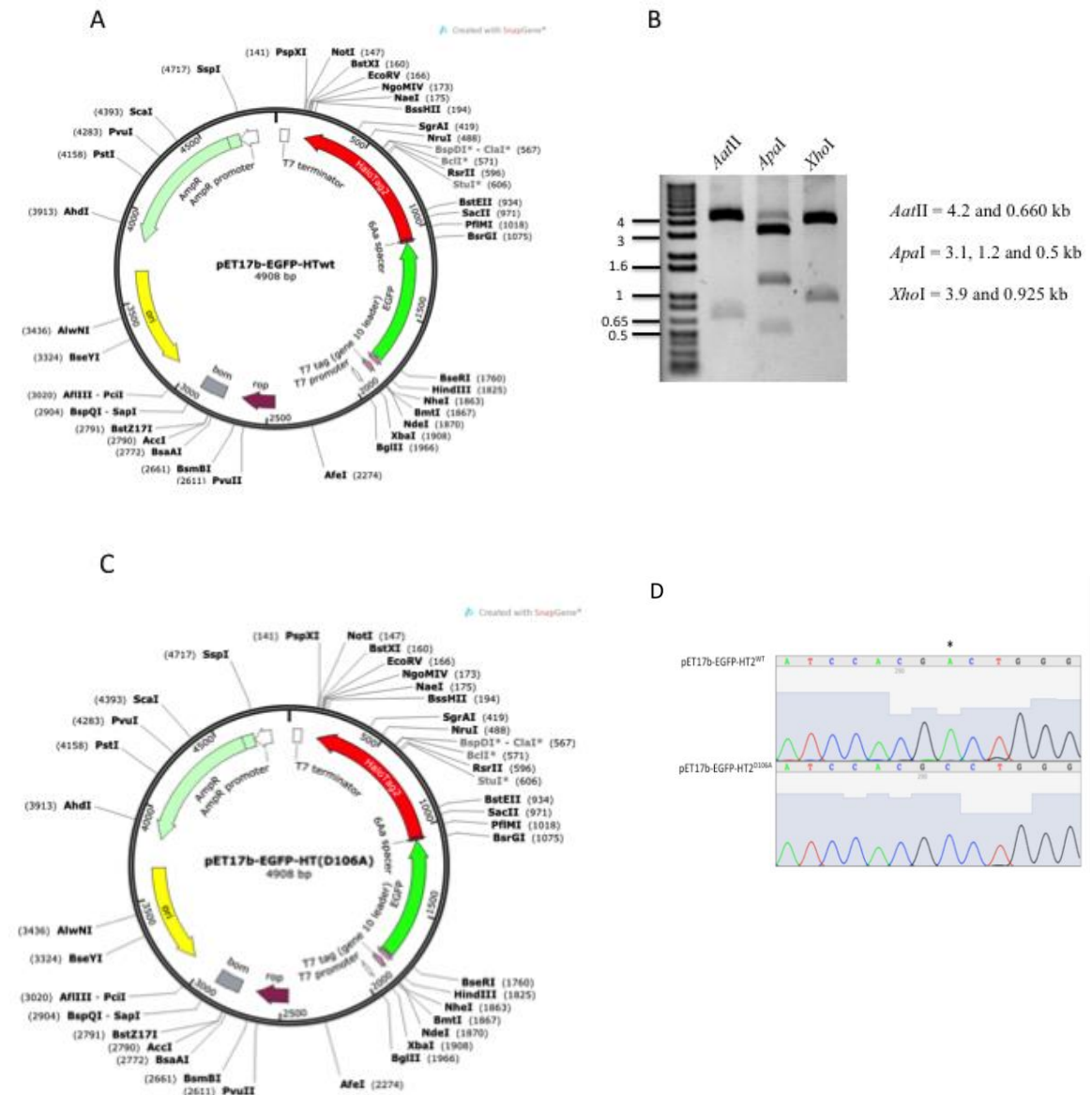


**Figure 4.1: Plasmid maps of pET17b carrying HaloTag<sup>WT</sup> and HaloTag<sup>D106A</sup> mutant fragment.** (A) pET17b plasmid containing EGFP-HT<sup>WT</sup> under the T7 promoter and terminator regulatory elements. (B) pET17b-EGFP-HT<sup>WT</sup> plasmid digested with *Aat*II, *Apa*I and *Xho*I enzyme and resolved by 0.8% agarose gel electrophoresis. (C) pET17b plasmid carrying HaloTag fragment having mutation D→A at amino acid residue 106. (D) Raw chromatograms showing the sense-strand sequence data of HT<sup>WT</sup> and HT<sup>D106A</sup>; an asterisk marks the mutated nucleotide.

#### 4.1.2 EGFP-HT2 protein expression, Western blot detection and fluorophore labeling

To test the function of the HaloTag moiety, the same dilutions of protein extract were reacted with tetramethyl rhodamine (TMR)-labeled haloalkane ligand. The TMR-ligand protein extract reactions were denatured and resolved by SDS-PAGE. Fluorescence imaging of the SDS-PAGE gel demonstrated a signal corresponding to a protein complex of the expected size of ~61.8 kDa for EGFP-HT wild type. In contrast, no signal was detected from EGFP-HT<sup>D106A</sup> protein reactions (**Figure 4.2A**). Total soluble proteins were isolated from EGFP-HT2 expressing transformed *E. coli* BL21 (DE3) bacterial host. 10, 5 and 1 µg of each dilution of protein extract was used for Western detection. SDS-PAGE was performed and membrane transferred electrophoretically. When probed with anti-GFP primary antibody, a protein species of the size expected for full-length EGFP-HT2 fusion protein (~61.8 kDa) was observed for both EGFP-HT2 wild type and mutant (**Figure 4.2B**). This result confirmed that, in *E. coli*, both EGFP-HT<sup>WT</sup> and EGFP-HT<sup>D106A</sup> fusion genes were able to be expressed as a full-length protein.



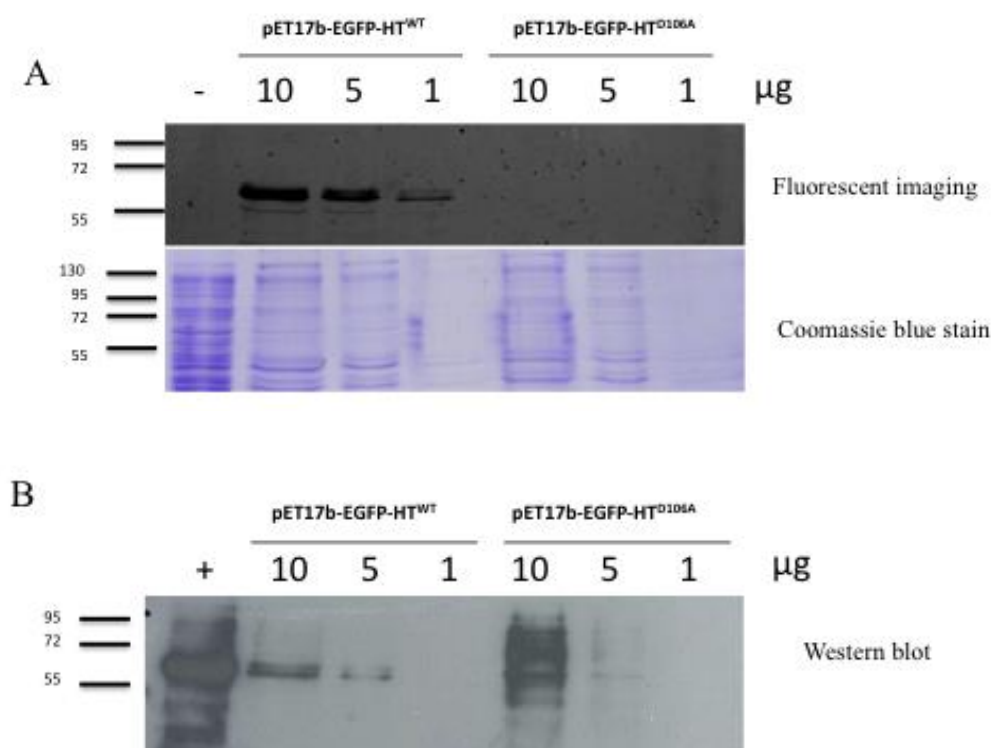


**Figure 4.2: Detection of EGFP-HT fusion protein by Western blot and fluorophore labeling.** (A) 10, 5 and 1 μg of total protein expressing EGFP-HT fusion was labeled with 1 μM of TMR fluorophore ligand and performed SDS-PAGE separation. The migrations of prestained protein marker are indicated on the left. Typhoon 9410 imager was used to scan the SDS-PAGE gel at  $E_{ex} = 532$  nm and  $E_{em} = 580$  nm wavelength. (B) The expression of EGFP-HT<sup>WT</sup> and EGFP-HT<sup>D106A</sup> fusion protein detected using Western blot by anti-GFP primary antibody. The migrations of prestained protein marker are indicated on the left. The migration of the ~61.8 kDa protein band expected for EGFP-HT is marked by an arrow. The lane marked + is a positive control of EGFP-HT cell lysate.

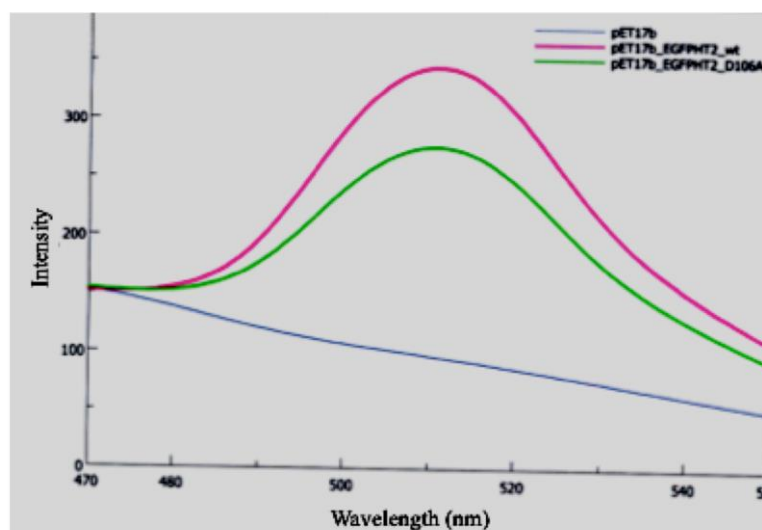
#### 4.1.3 Fluorometric assay and effect of hydrophobic ligands on EGFP-HT fusion protein stability

HyT13 hydrophobic ligand was previously shown to reduce thermal stability when complexed with HaloTag fusion protein *in vitro* (60). Therefore, it was

hypothesized that the complex of HyT13 and EGFP-HT2 could lead to reduced EGFP activity, which could be measured quantitatively using spectrofluorometry. Maximum emission for EGFP fluorescent protein was detected at 510 nm. Fluorescent intensity of the EGFP-HT<sup>WT</sup> fusion protein was higher than that of EGFP-HT<sup>D106A</sup> mutant protein (**Figure 4.3A**). Protein isolated from pET17b empty plasmid was used as a negative control in this experiment to establish the baseline fluorescence. 10  $\mu$ M of HyT13 ligand was incubated with 10  $\mu$ g of crude protein, and relative fluorescence intensity was measured using spectrofluorometry. Data from three independent experiments were combined and mean values were normalized for making a bar graph to quantify the expression of EGFP-HT<sup>WT</sup> and EGFP-HT<sup>D106A</sup> fusion protein and comparisons were made between HyT13 treated and untreated protein samples. (**Figure 4.3B**). pET17b expressing empty plasmid was used as a negative control for correcting the fluorescence background. Cells transformed with PR300 plasmid were used as a positive control, which expresses natural EGFP under constitutive L-lactate dehydrogenase promoter (p<sub>ldhL</sub>) derived from *L. sakei* (57). Protein fluorescence was compared between HyT13 treated and untreated protein samples. Data were obtained from three independent experiments for each protein, and raw fluorescence values were transformed by dividing with the mean value of negative control (background value). The fluorescence of the positive EGFP control was approximately 20 times higher than the EGFP-HT<sup>WT</sup> fusion protein for both HyT13 treated and untreated samples. Interestingly, the fluorescence of the total protein expressing EGFP-HT<sup>D106A</sup> fusion protein was two-fold less than EGFP-HaloTag<sup>WT</sup> fusion protein for both HyT13 treated and untreated samples. It was also observed that there were no significant differences between HyT13-treated and untreated protein samples for any protein tested. Therefore, HyT13 has no effect on EGFP fluorescence. One possible explanation for the lack of effect of HyT13 treatment on EGFP-HT<sup>WT</sup> fluorescence is that it did not conjugate efficiently under the conditions tested. Since HyT13 is hydrophobic, it may alter EGFP-HT<sup>WT</sup> fusion protein properties such that the ligand-protein complex could have altered mobility in SDS-PAGE, as it is well known that hydrophobic proteins have anomalous migration in SDS-PAGE (61). 10-fold dilutions of HyT13 and HyT36 ligand were made ranging from 0.1-10  $\mu$ M concentrations for coupling reaction with 10  $\mu$ g of total protein expressing EGFP-HT2, and standard

Western blot was performed. Chemiluminescent detection method was used for detecting EGFP-HT<sup>WT</sup> and EGFP-HT<sup>D106A</sup> fusion protein (~61.8 kDa expected size full-length) (**Figure 4.4 B and C**). The result shows that EGFP-HT<sup>WT</sup> was expressed at a higher level than EGFP-HT<sup>D106A</sup>, as shown by the intensity of a band at ~61.8 kDa of the expected size for full-length protein. The higher expression of EGFP-HT<sup>WT</sup> by Western is thus consistent with EGFP fluorescence experiments. Comparison of HyT13 treated with control protein revealed additional complexes of different mobility for EGFP-HT<sup>WT</sup> treated protein, although the pattern was inconsistent owing to spurious signal from protein overloading.

A



B

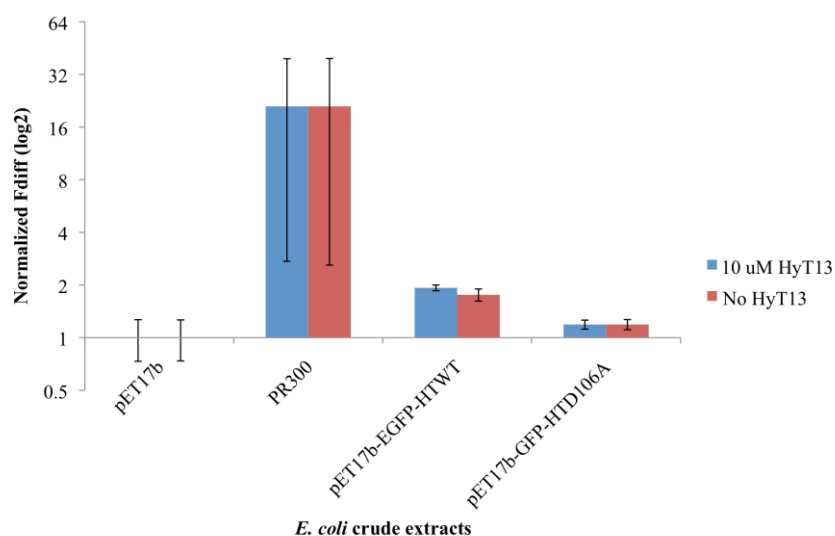


**Figure 4.3: Fluorometric assay for measuring the activity of EGFP-HT<sup>WT</sup> and EGFP-HT<sup>D106A</sup> fusion protein. (A)** Fluorescence intensity was compared between EGFP fused to HT<sup>WT</sup> or HT<sup>D106A</sup>. **(B)** Bar graph showing the comparisons of the transformed mean background-corrected fluorescence among HyT13 treated total protein with untreated protein. Three independent experiments were performed, and error bars represent normalized coefficient of variance.

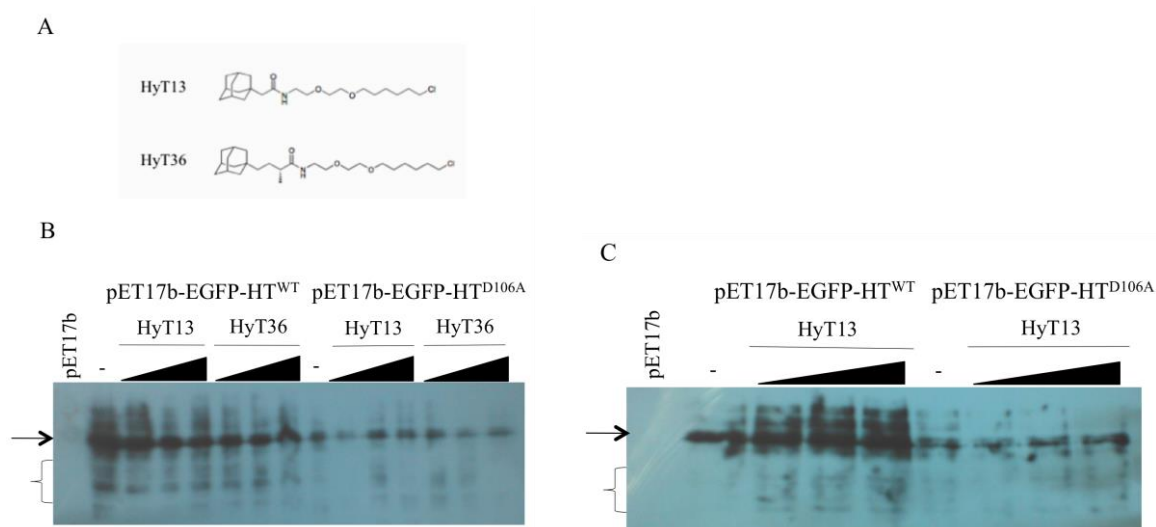


**Figure 4.4: Western blot of EGFP-HT fusion protein coupled with HyT13 ligand**

(A) Chemical structures of HyT13 and HyT36 hydrophobic chloroalkane ligand containing adamantine based moiety (48). (B and C) Western blot detection of total protein from cells expressing EGFP-HT2 fusion protein treated with various dilutions of HyT13 and HyT36 hydrophobic ligands. Concentrations of the ligands were varied from 0.1, 1 and 10  $\mu$ M. Blank (no ligand) control lanes are marked by – above the lanes. ~61.8 kDa expected full-length EGFP-HT protein was detected (marked by the arrow) by chemiluminescence method using anti-GFP primary antibody. Additional bands of faster mobility were also observed, as indicated by the brace.

## 4.2 Analysis of DHFRTS-HaloTag fusion protein activity in *E. coli*

Dihydrofolate reductase thymidylate synthase (DHFRTS) is an essential enzyme in the folate pathway of *Plasmodium* parasite, which is important for pyrimidine biosynthesis and its survival. The aim of this research was to characterize the effect of the C-terminal HT fusion to *Plasmodium falciparum* DHFRTS reporter enzyme in *E. coli*. The advantages of DHFRTS reporter protein are that any effect of HT fusion protein on DHFRTS activity can be observed by enzyme assay and functional complementation test. Crude extract from *E. coli* was isolated and DHFR activity was measured using spectroscopy. TMR ligand labeling was performed for detecting full-length DHFRTS-HT protein. Growth of *E. coli* was also measured by

functional complementation assay in a  $\Delta thyA \Delta folA$  double knockout (DKO) cell line to validate DHFRTS-HT fusion protein activities.

#### **4.2.1 Recombinant plasmid construction, heterologous expression of DHFRTS-HT fusion protein and DHFR activity analysis**

The DHFRTS-HT protein-coding gene was cloned into pET17b derived recipient vector, which maintains low-medium copy numbers and has a T7 inducible promoter to drive expression of target gene. *E. coli* BL21(DE3) bacterial host carrying pET17b-DHFRTS-HT vector was induced by IPTG for expressing DHFRTS-HT fusion protein.

As a positive control, pET17b-DHFRTS-His6x vector was used. This plasmid drives expression of active 6x His-tagged DHFRTS protein to a level sufficient for complete complementation of DKO growth (P. Shaw, unpublished data, personal communication). 10  $\mu$ l of soluble fraction expressing DHFRTS-HT fusion protein was added into the DHFR activity assay reaction. In the reaction, NADPH (nicotinamide adenine dinucleotide phosphate) was added as cofactor, and DHF (dihydrofolate) was used as a substrate. Mechanistically, DHFR enzyme catalyzes the reaction by transferring a hydride ion from NADPH to DHF. Therefore, DHF is reduced to become THF (tetrahydrofolate), and NADPH is oxidized to become NADP<sup>+</sup>. Using a spectrophotometer at 340 nm absorbance, enzyme activity is monitored by the decrease of NADPH to NADP<sup>+</sup>. When DHFR activity is high, more NADPH is converted to NADP<sup>+</sup> and rate of conversion (OD/min) will be higher. Three different fusion tags (HT2, HT7 and 6x His) were fused to the C-terminus of DHFRTS protein coding region. Student's t-tests were performed with three independent replicates for each protein activity. Insignificant differences in measured activity of protein extract between untransformed DKO and DHFRTS-HT2 expressing cells indicate that the latter has no DHFR activity above baseline. In contrast, the specific activity of DHFRTS-HT7 is significantly higher than DKO or DHFRTS-HT2 fusion protein, indicating that DHFRTS-HT7 does have some DHFR activity. However, DHFR activity of the 6x His fusion tag extract was significantly higher than DHFRTS-HT (p<0.05) (**Figure 4.5**). Therefore, this finding indicates that C-terminal HaloTag has a negative impact on the specific activity of DHFRTS enzyme.

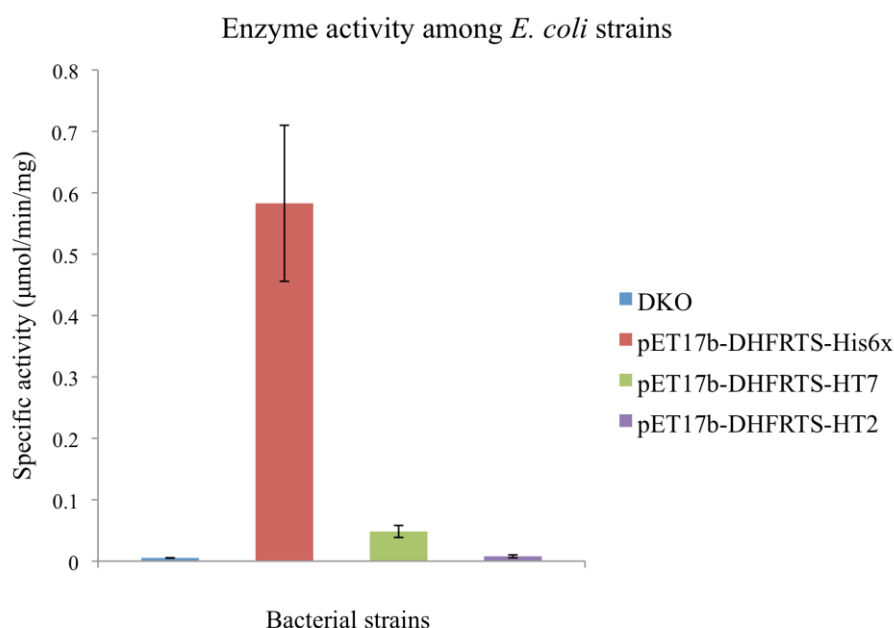


**Figure 4.5: Comparison of enzyme specific activity among bacterial strains.**

Bar graph shows the comparisons of DHFR specific activity among the soluble fraction isolated from the bacterial strain expressing DHFRTS-HT fusion protein with different C-terminal fusion tags. DHFR specific activity with the C-terminal 6x His tag is significantly higher than those from DHFRTS-HT2 and DHFRTS-HT7 fusion proteins (student t-test; and p-value <0.05). (Experiments were triplicate n = 3, error bars considered as a standard error of mean). (Calculated p-value is given DKO Vs 6x His is 0.010, DKO Vs HT7 is 0.011, DKO Vs HT2 is 0.319, 6x His Vs HT7 is 0.013, 6x His Vs HT2 is 0.010, HT2 Vs HT7 is 0.015)

#### 4.2.2 Detection of TMR labeled full length DHFRTS-HT protein

To test the activity of HT fusion protein, 1 μM of TMR ligand was used to perform the coupling reaction with the bacterial crude extract expressing full-length DHFRTS-HT. EGFP-HT2 protein extract was used as a control (**Figure 4.6A and 4.6B**). A signal corresponding to full-length protein was observed for DHFRTS-HT7 (~107 kDa), in addition to other bands of higher mobility. These smaller proteins are probably N-terminal truncations of DHFRTS-HT7. Truncated protein species are also observed when untagged DHFRTS is expressed in *E. coli* (62). This result indicates that DHFRTS-HT7 is active for the HT7 moiety.

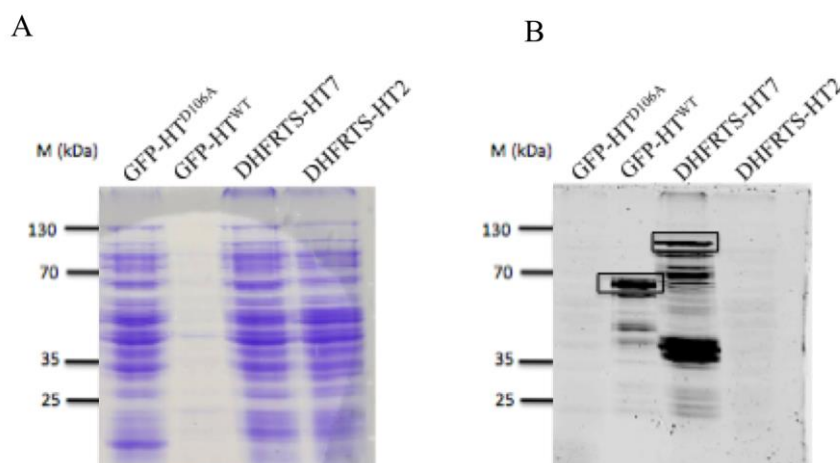


**Figure 4.6: TMR labeling of full-length DHFRTS-HT7 and DHFRTS-HT2 protein.** (A) Each lane of SDS-PAGE gel showed the protein loading which was measured by Bradford assay. (B) TMR labeled crude extract isolated from bacteria. 20  $\mu$ g of crude protein was loaded from cells expressing EGFP-HT<sup>D106A</sup>, DHFRTS-HT2 and DHFRTS-HT7 fusion proteins. As a positive control, 1  $\mu$ g of EGFP-HT<sup>WT</sup> protein extract was used to determine the specificity of TMR ligand binding. In TMR labeling experiment, full-length DHFRTS-HT7 protein was detected at ~107 kDa marked with black square block. No DHFRTS-HT2 fusion protein was detected by TMR labeling. EGFP-HT<sup>WT</sup> was used as a positive control which gives a ~61.8 kDa size, and no signal was detected from EGFP-HT<sup>D106A</sup> negative control. M designates page ruler prestained molecular weight marker (Thermo scientific).

#### 4.2.3 Functional complementation among the bacterial strains

Complementation test was performed in order to observe the effect of fusion tag at the C-terminus on DHFRTS activity. All three plasmids carrying DHFRTS with C-terminal fusion tag were transformed into the DKO *E. coli* bacterial cell line deficient in *thyA* and *folA* genes (63). In bacteria, *thyA* and *folA* encode TS and DHFR enzyme, respectively. Without *thyA* and *folA* genes, the bacterial TS and DHFR enzymes are unable to be synthesized. So, the DHFR and TS activities can be complemented either by introducing a *Plasmodium* bifunctional DHFR-TS gene via plasmid DNA, or adding exogenous thymidine into bacterial growth media (*E. coli* can salvage pyrimidine to overcome defects in de novo pyrimidine synthesis). In this



experiment, *E. coli* expressing full-length *P. falciparum* DHFRTS fusion protein from extra chromosomal plasmid complemented DHFR and TS enzyme activity. Growth of the *E. coli* was measured for transformants expressing DHFRTS protein fused with C-terminal HT2, HT7 and 6x His tag. After eight hours, it was observed that DHFRTS-6x His fusion protein fully complemented the DKO cells, since the growth reached a level comparable to thymidine-complemented  $\Delta thyA \Delta folA$  cells.

*E. coli* DKO strain expressing DHFRTS-HT7 protein showed partial complementation (t-test comparing 8 h growth of DKO with DHFR-HT7 on LB;  $p < 0.05$ ). In contrast, DHFRTS-HT2 fusion protein failed to complement the knockout cells (t-test comparing 8 h growth of DKO with DHFR-HT2 transformed DKO on LB media,  $p > 0.05$ ) (**Figure 4.7**).

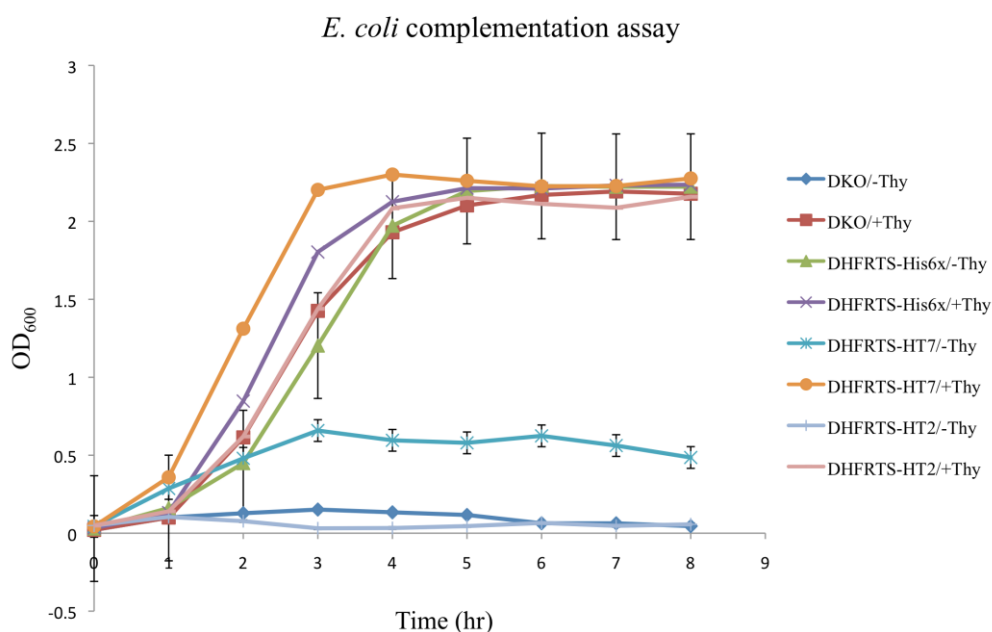


**Figure 4.7: Complementation tests among the *E. coli* strain expressing DHFRTS enzyme.** Bacterial growth response was measured in the prototrophic media is supplemented with thymidine and growth was observed among the *E. coli* strain having the recombinant vector with or without DHFRTS enzyme. However, in media supplemented with thymidine, DHFRTS enzyme was fully complemented upon 6x His fusion tag ( $p < 0.05$ ) and growth was saturated at 8 hours. (Calculated p-value is given

6x His Vs DHFRTS-HT7 is 0.0115, 6x His Vs DHFRTS-HT2 is 0.0006, DHFRTS-HT7 Vs DHFRTS-HT2 is  $8.828 \times 10^{-06}$ , DKO Vs DHFRTS-HT2 is 0.0541)

### 4.3 Activity of HaloTag on toxic protein

The HT:HyT13 inducible protein knockdown system works best with the earlier version of HaloTag (HT2) as a fusion protein component (48, 60). The ability to control fusion protein degradation by hydrophobic tagging may also depend on the inherently unstable character of HT2 protein for enhancing the degradation of target protein. It was shown that the structural instability of HT2 is the principal characteristic that improved the degradation of the fusion protein more rapidly upon binding of HyT13 hydrophobic compound (60). These data led us to the hypothesis that further reduction of HT2 protein stability could lead to even more efficient attenuation of protein level upon complex formation with HyT13 ligand. A similar approach has been pursued for improving the FKBP/Shld system, in which less stable FKBP variants can give improved knockdown efficiency (40). The toxic protein from a toxin-antitoxin (TA) module system was explored for selecting unstable variants of HT2. Expression of toxic proteins in TA modules in bacteria is very low and tightly regulated by antitoxin (64). In this part of the research, toxic protein is used to isolate HT variants. The goal is to generate variants of HT2 fused to the N-terminus of the toxic protein. Unstable HT2 variants will trigger the degradation of toxic protein fusion by ATP-dependent protease (65) and allow the growth of bacteria. On the other hand, toxic protein fused with stable HT2 variants will lead to the accumulation of toxic protein and inhibit the cell growth. There are several genes encoding toxic protein such as CcdB, Gef and MazF, and their expressions can be controlled under pBAD promoter (66). In this experiment, pBAD expression system was chosen for controlling CcdB bacterial toxin expression in which encoded by the ccd operon of F plasmid in *E. coli* (64). CcdB is a stable and potent toxin that targets the essential DNA gyrase enzyme and dismantles the positive supercoiling of DNA in front of the replication fork leading cell death to *E. coli* due to stalling the DNA replication and transcription (67). 8.7 kDa CcdA and 11.7 kDa CcdB small protein were encoded from ccd operon in *E. coli*. Naturally, CcdB toxin is neutralized by CcdA antitoxin via non-

covalent complex formation that keeps the replication process functional in the bacterial cell. CcdB gene is also used as a tool for cloning genes in plasmids. In this application, disruption of CcdB open reading frame by the insertion of any external DNA fragment allows the growth of positive recombinants, and all non-recombinants are killed (69).

#### **4.3.1 Plasmid construction and TMR labeling of full-length CcdB-HT fusion protein**

The vector for expression of CcdB-HT protein in *E. coli* is from the pBAD family that includes medium copy number plasmids with an araC inducible promoter to drive expression of target protein. TMR labeling of bacterial crude extract expressing CcdB-HT fusion protein was performed in order to observe the functional HaloTag after CcdB toxic fusion. *E. coli* expressing CcdB-HT fusion protein was induced by 0.1% L-arabinose and 10 µg of crude extract was treated with 1 µM of TMR fluorescent ligand and resolved by SDS-PAGE (**Figure 4.8A**). SDS gel was scanned in Typhoon imager at specific excitation and emission wavelength ( $E_x/E_m = 532/580$ ) at which TMR labeled CcdB-HT fusion protein was detected (**Figure 4.8B**).

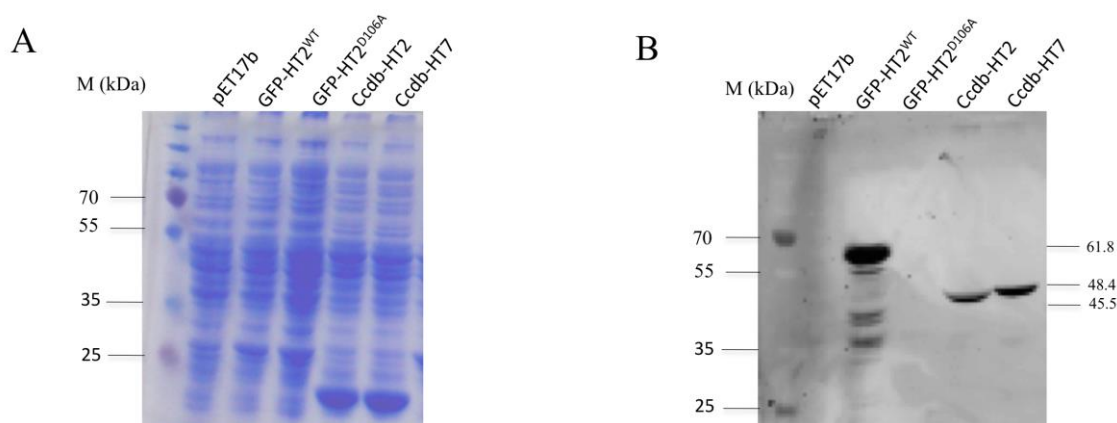


**Figure 4.8: Detection of TMR labeled CcdB-HT fusion protein.** (A) Coomassie stained SDS-PAGE showed the normalized loading of proteins. (B) CcdB-HT2 and CcdB-HT7 protein was detected approximately at 45 kDa and 48 kDa respectively. Crude protein isolated from *E. coli* pET17b empty plasmid and EGFP-HT2<sup>D106A</sup> was used as negative control. Therefore, EGFP-HT<sup>WT</sup> used as a positive control, which was detected at ~61.8 kDa. M was designated as a molecular marker.

#### 4.3.2 Bacterial strain expressing CcdB-HT fusion protein

To characterize the activity of CcdB-HT fusion protein, expression plasmid carrying CcdB-HT fusion gene was transformed into *E. coli* DH5 $\alpha$  cell line and over expressed by addition of with 0.1% L-arabinose.  $A_{600}$  was measured every hour for the total of 8 hours. As a control to show that a toxic protein expressed from pBAD plasmid can inhibit bacterial growth, *E. coli* DH5 $\alpha$  was transformed with pBAD-EviB. In agreement with published work (66), the growth of cells transformed with this plasmid is inhibited upon arabinose induction. In contrast, growth of cells was unaffected after induction for cells transformed with pBAD-CcdB-HT2, pBAD-CcdB-HT7 and pBAD33 (**Fig. 4.9**). Although CcdB-HT2 and CcdB-HT7 were expressed as a full-length proteins (Fig. 4.8), *E. coli* growth experiments showed that the toxic property of CcdB protein was inactivated.

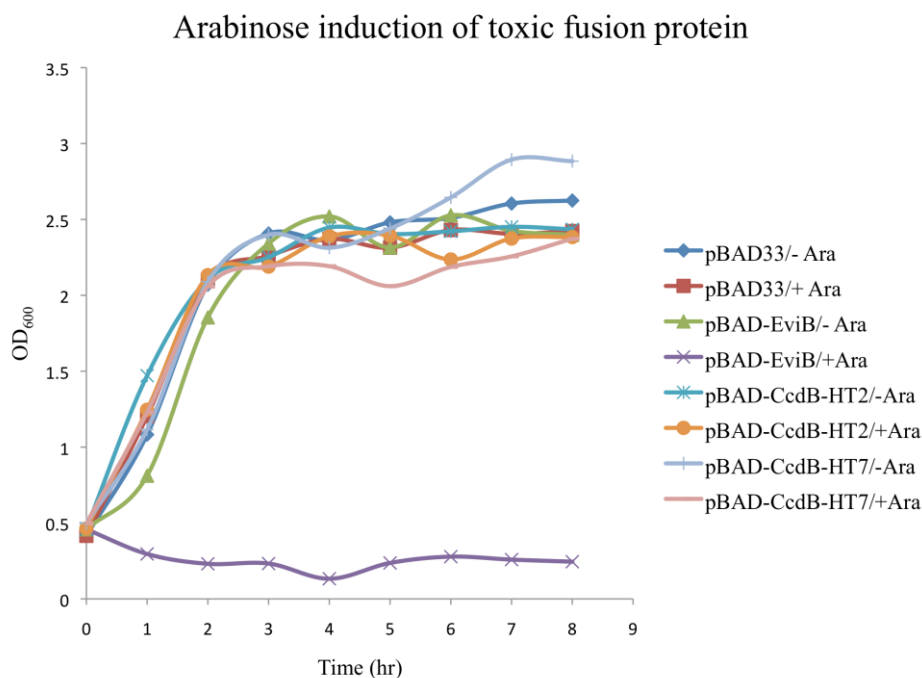


**Figure 4.9: Growth curve of *E. coli* expressing CcdB-HT fusion protein.** Cell lines were induced by 0.1% arabinose and compared with uninduced cell line expressing CcdB-HaloTag fusion protein (pBAD-CcdB-HT2). *E. coli* expressing phiX E gene (pBAD-EviB) used as a positive control for toxic protein function for which expression was tightly regulated under arabinose promoter (66).

#### 4.4 HaloTag utilities in *Plasmodium*

HT7 has been used to detect the localization of a protein important for gametocyte maturation in *P. falciparum* (56). HaloTag could thus be applied as a decon tool in *P. falciparum* for studying essential protein, in which HaloTag fusion protein expression is controlled by highly specific and non-toxic cell permeable hydrophobic ligands (48, 60). In this part of research, *Plasmodium* DHFRTS was used to test the HaloTag mediated knockdown strategy in *P. falciparum*. The ultimate goal is to test whether expression of a DHFRTS-HT fusion protein can be controlled by HyT13 ligand, in which addition of ligand to the transgenic parasite is expected to lead to knockdown DHFRTS protein, which would affect sensitivity to antifolate drugs targeting DHFR. Previously, it was shown that knockdown of *Pf*DHFRTS expression

by *glmS* ribozyme can sensitize parasites to the antifolate drug pyrimethamine (30). To utilize HaloTag in asexual stages of *P. falciparum*, a transgenic vector was constructed with HT7 C-terminal to DHFRTS. This plasmid was transfected into parasites and transgenic parasite containing the DHFRTS-HT7 gene were confirmed by gene specific PCR. Localization study of DHFRTS-HT7 was performed in transgenic parasites using fluorescent-labeled ligand.

#### **4.4.1 Transgenic plasmid construction which contains *Pf*DHFRTS-HT fusion protein coding region**

HT7 gene was subcloned into the C-terminal position of *Pf*DHFRTS via *KpnI/PstI* restriction sites and the integrity and orientation of *Pf*DHFRTS-HT7 sequence confirmed by restriction mapping and sequencing. The expression of *Pf*DHFRTS-HT7 fusion protein is regulated under heat shock protein 86 (Hsp 86), a constitutive parasite promoter. The vector also contains a blasticidin resistant selection marker for selecting positive parasite transfectants. Another parasite transfection vector was constructed carrying the HT2 sequence in place of HT7, in which the same *KpnI/PstI* sites were used for cloning HT2 sequence.

#### **4.4.2 Confirmation of positive transfectant in *Plasmodium falciparum***

Genomic DNA was isolated from transgenic parasite and positive transfectants identified by PCR using specific primers to amplify the *Pf*DHFRTS-HT7 sequence from the episomal vector. PFD-03LS-EGFP genomic DNA isolated from different transgenic line was used as a negative control (**Figure 4.10, lane 4-6**). PF-TS forward and Dhfr-3-UTR reverse primer pair was used to specifically amplify ~1kb sequence from 5'-TS and DHFR located at 3' UTR of the *P. falciparum* PFD0830w locus on chromosome 4 (**Figure 4.10, lane 1-3**) and also used as a positive control for episomal *Pf*DHFRTS-HT7 vector (**Figure 4.10, lane 10-12**) The Dhfr-*Bam*HI forward HaloTag-*Pst*I reverse primer amplified the expected ~2.7kb of the DHFRTS-HT fragment from the *Pf*DHFRTS-HT7 transfected parasites only and not the negative gDNA control PFD-03LS-EGFP from parasites lacking HT7 gene (**Figure 4.10, lane 8-9**), indicating that the *Pf*DHFRTS-HT7 plasmid had successfully transfected into *P. falciparum* 3D7 cell line and was maintained as an episomal vector. In another

experiment, no parasites were obtained after drug selection from transfection with plasmid expressing DHFRTS-HT2 fusion protein.

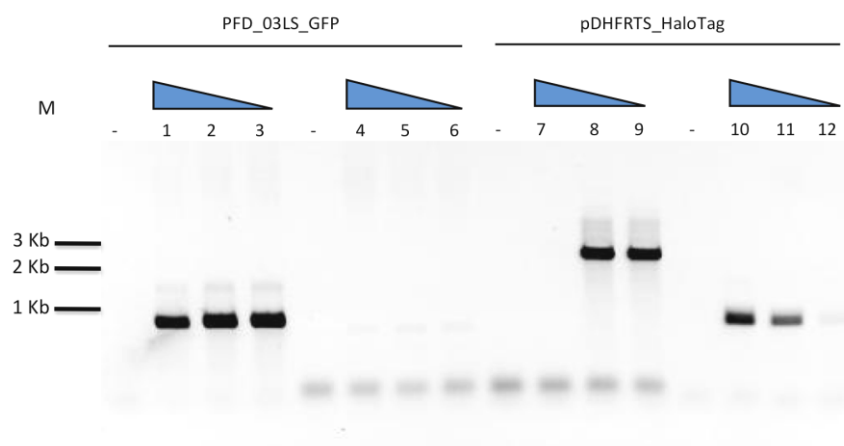


**Figure 4.10: Identification of *P. falciparum* transgenic parasite carrying *PfDHFRTS-HT7* episomal transfection vector.** Lane 1 to 3 and 10 to 12 represent the reaction with primers specific for PFD0830w locus (positive control primer pair). Lane 4 to 6 and 7 to 9 represent the reaction with primers specific to DHFRTS-HT7. gDNA template was varied from 50, 30 and 10 ng. Blank (no template) control lanes are marked by – above the lanes. (Ladder 1kb plus, Invitrogen).

#### 4.5 HaloTag expression in *P. berghei* parasite

*P. berghei* is a species of *Plasmodium* that infects rodents and is also useful for malaria research, in particular *in vivo* studies requiring a mammalian host. Previously, it was reported that HT2 degron could be controlled *in vivo* in mice to reduce live tumor by injection of hydrophobic ligand (48). Hence, HT2 could be useful for controlling expression in *P. berghei* infected mice since the hydrophobic ligand has no apparent *in vivo* toxicity at the doses needed to induce HT2 fusion-protein degradation. So, enhanced green fluorescence protein (EGFP) was used as a reporter protein fused to HT2 that can be controlled *in vivo* by HyT13 ligand. In parasite expression plasmid, *P. berghei eef-1α* constitutive promoter is controlled the expression of EGFP-HT2 fusion protein in blood stage parasites. The transfection

plasmids also have a Tg-DHFRTS selectable marker for selecting positive transgenic parasite and homologous integration sequence which integrates the entire plasmid into the non-essential *ssu-rrna* in *P. berghei* genome. Transgenic parasites were selected and limiting dilution was required for establishment of clonal lines. Thereafter, integration of transgenic vector was confirmed by PCR. Expression of HT2 gene was confirmed by RT-PCR.

#### **4.5.1 Generation of transgenic parasites expressing EGFP-HT fusion protein**

Two parasite expression vectors carrying EGFP-HT2 fusion gene was made in order to introduce them into the *P. berghei* genome (**Fig. 4.11A**). The pL0017-EGFP-HT<sup>WT</sup> has the wild-type HT2 sequence, whereas pL0017-EGFP-HT<sup>D106A</sup> has HT2 sequence mutated to express D106A mutant protein, which cannot form covalent complexes with haloalkane ligand (48). Single crossover homologous integration have occurred at the non-essential *ssu-rrna* locus in order to introduce these plasmid vectors which generated transgenic parasites *PbEGFP-HT<sup>WT</sup>* and *PbEGFP-HT<sup>D106A</sup>* (**Figure. 4.11 B and C**).

#### **4.5.2 Confirmation of transgenic DNA integration in transfectants**

Genomic DNA was isolated from *PbEGFP-HT<sup>wt</sup>*, *PbEGFP-HT<sup>D106A</sup>*, *PbEGFP* transgenic parasites and *PbANKA* reference parasite. Isogenic clonal lines with integration of transgenic DNA at the *c* or *d-rrna* unit were verified by PCR (**Figure. 4.11D**). Integration at the 5' end was confirmed using the 5'-*ssuFp* forward (P1) and 5'-*ssuRp* reverse primer (P3) pair which amplified a ~2.8kb product from the transgenic lines. 3' end integration was confirmed using 3'-*ssuFp* forward (P2) and 3'-*ssuRp* (P4) primers which amplified a ~2.1kb product from transgenic lines (**Figure 4.11D**). In both of these experiments, no product was detected from the *PbANKA* negative control. HaloTag specific primers HT2-Fp forward and HT2-Rp reverse primers amplified a 920 bp as expected from *PbEGFP-HT<sup>WT</sup>*, *PbEGFP-HT<sup>D106A</sup>* parasites, but not from *PbEGFP* or *PbANKA* (**Figure 4.11E**). As a control, GS and ALAS genes were PCR amplified from all four parasite DNA samples (**Figure 4.11F**).



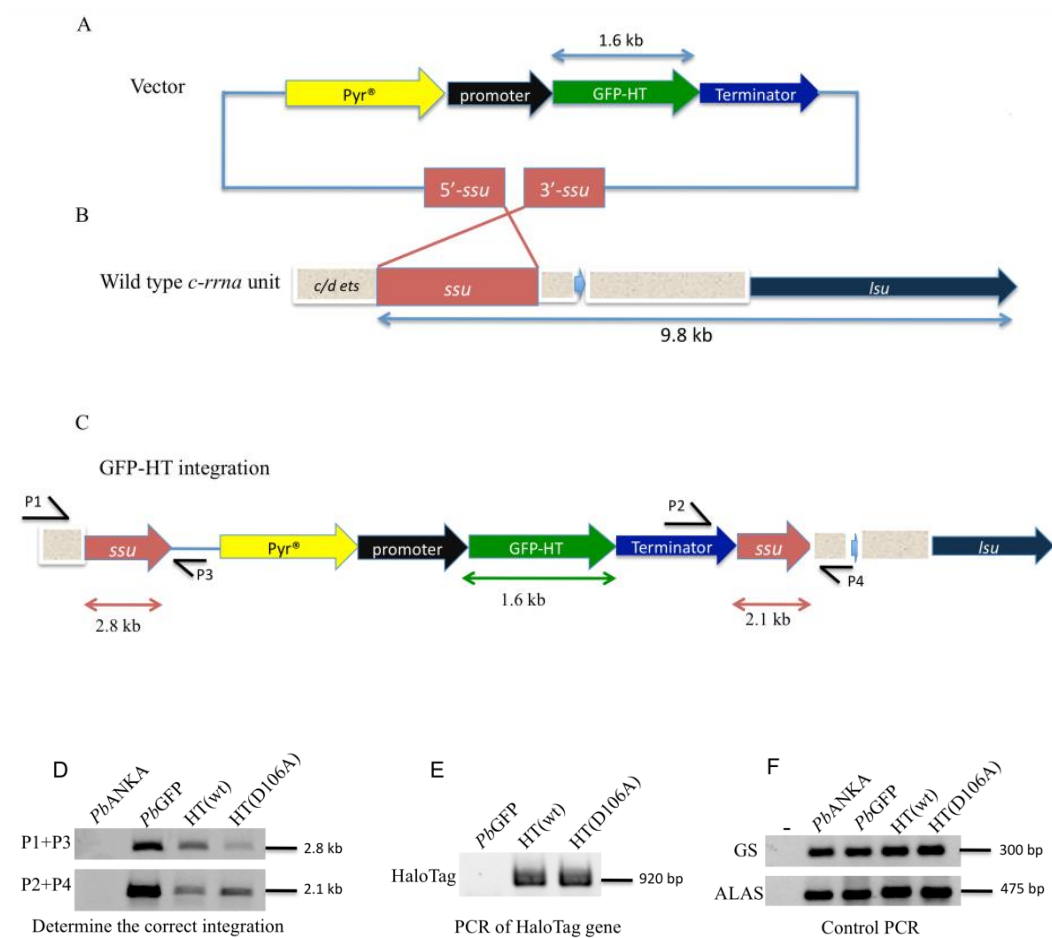


**Figure 4.11: Construction of *PbEGFP-HT* parasites.** (A) The transgenic vector carrying EGFP-HT fusion gene was used for integration into *c* or *d-rRNA* unit of *P. berghei* genome. Vectors were linearized at unique *ApaI* restriction site having *d-ssu-rRNA* homologous targeting sequence with *P. berghei* genome. Plasmids were also have *tgdhfr-ts* marker (Pyr<sup>R</sup>) for selection of transgenic parasites against pyrimithamine drug. EGFP-HT fusion gene is cloned between *eef-1α* promoter and 3'-UTR sequence of *Pbdhfr-ts*. (B) Graphical representation of the target site in *P. berghei* genome where transfection plasmids were integrated. (C) Representation of integrated transgenic plasmid carrying selectable marker Pyr<sup>R</sup> and EGFP-HT2 fusion cassette. Arrows indicate the expected sizes of products confirming correct integration at the *ssu* unit by PCR. (D) PCR was performed to show the presence of (E) HT2 gene and (F) GS and ALAS genes.

### 4.5.3 Expression of transgenic EGFP-HT at the RNA level

After parasitemia reached ~15%, blood was collected from the mouse and total RNA was extracted. cDNA was prepared from transgenic parasites to assess the expression of EGFP-HT2 fusion at the parasite transcript. RT-PCR was performed using 5'-HT2-Fp and 3'-HT2-Rp primers, which specifically amplified the 920 bp HaloTag gene sequence (**Figure 4.12**) from cDNA extracted from the parasite lines bearing EGFP-HT fusion genes. However, no PCR product was generated with this primer pair from *PbANKA* and *PbGFP* parasite samples, or from samples lacking reverse-transcriptase enzyme (-RT). The control GS-Fp forward and GS-Rp reverse primers amplified a 300 bp glutathione synthetase gene product from all parasite cDNAs, thus verifying the integrity of cDNA preparations.

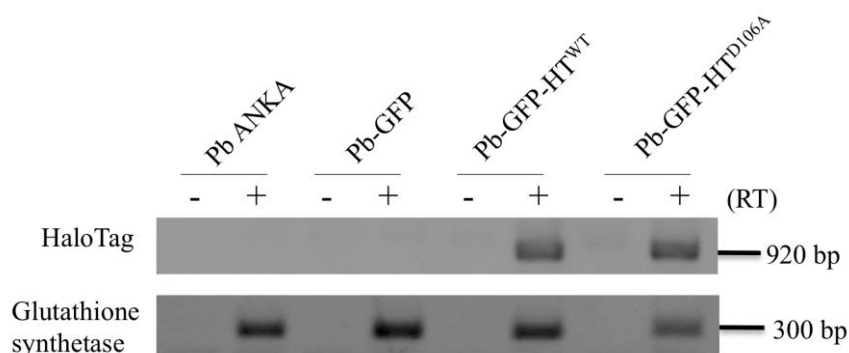


**Figure 4.12: Detection of HaloTag transcript by Reverse Transcription PCR (RT-PCR).** cDNA was prepared by oligo(dT<sub>21</sub>) primed reverse transcription from total parasite expressing EGFP-HT<sup>WT</sup> and EGFP-HT<sup>D106A</sup> mRNA. Control reactions lacking reverse-transcriptase enzyme were performed in parallel (lanes marked -). The sizes of expected product for HT2 (920 bp) and Glutathione synthetase (GS, 300 bp) are indicated on the right.

### 4.5.4 Western analysis of EGFP expression in transgenic parasites

Based on Bradford colometric assay measurement, more than 30 µg of total parasites protein were isolated and SDS-PAGE was performed using 30 µg of total parasite protein in which subsequently subjected to perform Western blot. A positive control, 10 µg of total protein from bacteria expressing EGFP-HT<sup>WT</sup> was

used. No Western signal was observed in the lanes loaded with protein extracted from parasites, despite the transfer of protein onto the membrane as shown by Ponceau-S staining (**Figure 4.13**).

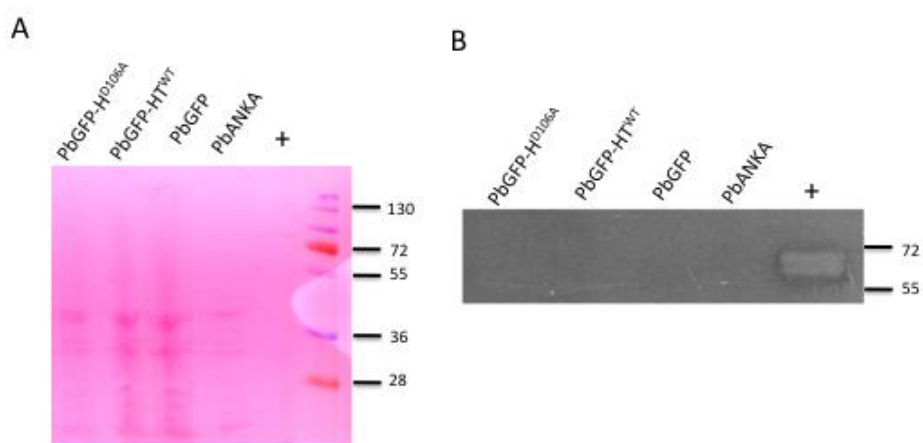


**Figure 4.13: Parasite protein transferred into PVDF membrane.** (A) Ponceau S staining of PVDF membrane showed the protein loading and transfer. (B) Chemilluminescence detection of EGFP-HT2 protein. 5  $\mu$ g of EGFP-HT2 protein expressed in bacteria used as a positive control. Anti-HaloTag primary antibody (Promega) was used to detect the ~61.8 kDa target protein band.

## CHAPTER V

### DISCUSSION

HaloTag (HT) is an engineered bacterial dehalogenase enzyme derived from *Rhodococcus rhodochrous* species, which is available as HT2 and HT7 variants. HT7 is a molecular tag useful for protein studies such as *in vivo* protein localization (70), *in vitro* purification (71) and protein: protein (72) and protein: DNA interaction (73). Recently, HT2 has also been used to control protein expression. Specific cell permeable bifunctional chloroalkane ligand was designed that contains a synthetic hydrophobic moiety. Upon binding to HaloTag protein, the hydrophobic part is exposed to the protein surface, which mimics the partially denatured state of protein to activate cellular UPR for protein degradation. This application of HT2 has been demonstrated for controlling reporter protein *in vitro* mammalian cell culture and in mice (48). As a fusion protein, the function of HaloTag in *E. coli* and *Plasmodium* was reported in this research. EGFP was used as a reporter protein fused to HT2 in both *E. coli* and *P. berghei* host. DHFR<sup>TS</sup> was used as another reporter protein fused to HT2 and HT7 in *E. coli* and *P. falciparum*. CcdB was expressed as a fusion protein with HT2 and HT7 in *E. coli*.

#### 5.1 EGFP-HT2 function in *E. coli*

The D106A mutation was successfully created in HT2 to make EGFP-HT2<sup>D106A</sup>, which was used as a control for TMR labeling experiment in order to test the functional specificity of wild-type HT2 when fused to EGFP (EGFP-HT2<sup>WT</sup>). In *E. coli*, expression of both wild type and mutant EGFP-HT2 have shown by the Western blot which detected ~61.8 kDa full-length EGFP-HT2. TMR HaloTag ligand formed a stable covalent complex with EGFP-HT2<sup>WT</sup>, but not EGFP-HT2<sup>D106A</sup> as expected. These experiments showed that the HT2 domain was fully functional when expressed as a fusion protein to EGFP in *E. coli*. Interestingly, the lower expression of the HT2

inactive mutant EGFP-HT2<sup>D106A</sup> was observed compared with EGFP-HT<sup>WT</sup>. The mutation of active-site residue in HT2 could have a dramatic effect on protein stability, which leads to lower levels of expression overall.

EGFP activity was demonstrated for both EGFP-HT2<sup>WT</sup> and EGFP-HT<sup>D106A</sup>, but the fluorescent activity of the latter was significantly lower. Perhaps, this active site mutation makes the HaloTag fusion protein less stable, but this requires more experiments for further validation; for example, comparison of thermal denaturation profiles of purified proteins. The difference in fluorescent activity reflected the difference in expression levels of the two proteins, as shown by Western blot. Ideally, the specific fluorescent activities should be tested using purified proteins to determine if the D106A mutation on HT2 has any effect on EGFP activity in the EGFP-HT2<sup>D106A</sup> protein. However, this was not practical because of the very low expression level. The effect of modulating HT2 structure on EGFP fluorescence was also tested *in vitro* by treatment of EGFP-HT2 fusion proteins with 10  $\mu$ M of HyT13 hydrophobic ligand. No significant changes were found in the protein treated with HyT13 compared with untreated soluble extract containing EGFP-HT2 fusion protein. The lack of an effect on EGFP was perhaps not surprising since HyT13 induces only a small change in protein thermal stability when complexed with HT2-fusion protein (60). *In vitro* proteasome assay needs to be performed to compare the degradation kinetics between EGFP-HT<sup>WT</sup> and EGFP-HT<sup>D106A</sup> fusion protein in the presence of ligand.

## 5.2 DHFRTS-HT2 and DHFRTS-HT7 function in *E. coli*

Since HT2 gave a low expression when fused to EGFP, HT2 was compared with HT7 when fused to a different protein partner, the *P. falciparum* DHFRTS protein. The fusion proteins were expressed in *E. coli* DKO strain deficient for DHFR and TS ( $\Delta folA \Delta thyA$ ). Functional complementation assay showed that DHFRTS-HT7 fusion protein partially complemented the  $\Delta thyA \Delta folA$  deficiency in *E. coli*, while HT2 fusion did not. The same pattern was observed in DHFR enzyme activity assay, in which DHFRTS-HT2 enzyme showed significantly lower activity than C-terminal 6x His-tagged DHFRTS enzyme, and DHFRTS-HT2 showed no

significant activity. So, these data suggested that HT2 and HT7 interfered with the activity of DHFR and/or expression level. The effect was more pronounced for HT2. TMR labeling experiments showed that most of the DHFRTS-HT7 labeled protein was truncated, while no signal was seen for DHFRTS-HT2. These results suggest that the main reason for lack of DHFR activity is instability and low-level expression of full-length intact DHFRTS-HT2 and DHFRTS-HT7. Previous comparisons of HT2 and HT7 fusion proteins have shown that HT7 is more thermostable and more resistant to chemical denaturants such as urea (53, 60). It is the intrinsic structural instability of HT2 protein relative to HT7 that allows it to act as an efficient degron upon binding with HyT13 hydrophobic ligand (60).

Although the expression of HT interferes with the function of DHFRTS enzyme, the protein expression might be improved either using another “solubilizer” tag (e.g. maltose binding protein) fused upstream of HT protein, or using a more soluble and more stable HT variant protein. A mutant library could be constructed containing HT variants fused to DHFRTS, which could be screened on the basis of complementation of DHFRTS function in the DKO cell. Highly soluble and stable HT mutants would complement more efficiently and thus outgrow DHFRTS-HT7 transformants.

### **5.3 CcdB-HT2 and CcdB-HT7 function in *E. coli***

Another aim of this thesis was to test whether further mutations of HT2 or HT7 could affect their ability to act as degrons for efficient knockdown of fusion proteins. CcdB toxic protein was used for testing HT fusion proteins by growth reporter assay. In this assay, it was expected that CcdB-HT2 and CcdB-HT7 fusion proteins would be sufficiently stable to accumulate as a toxic proteins and inhibit growth. Surprisingly, both full-length CcdB-HT2 and CcdB-HT7 proteins expressed strongly in *E. coli* as shown by TMR ligand labeling, but showed no toxic effect on growth. Mechanistically, CcdB protein targets bacterial intracellular gyrase-DNA complex, which blocks the passage of DNA polymerase and leads to breaks in double-stranded DNA followed by poisoning the bacterial cell (75). The function of CcdB toxin is critically dependent on the last three amino acid residues (Trp, Gly and Ile) of

the C-terminal part of CcdB protein, and any mutation of these residues causes CcdB to become inactive (74). DNA sequencing confirmed the expected sequence of CcdB-HT2 and CcdB-HT7, including the three critical amino acid residues of CcdB and in-frame fusion to HT2 and HT7. The full-length proteins were also clearly shown by TMR labeling. Structural studies have shown that CcdB protein forms a homodimer to DNA gyraseA subunit for exerting its toxic effect on bacteria (74, 75). Therefore, CcdB protein perhaps lost its killer activity due the extension of its C-terminal part by fusion to HaloTag that disrupts the dimer formation that is required for CcdB function. Other controls including expressing untagged CcdB protein and N-terminal Halo-tagged CcdB are required to identify possible interference caused by the HaloTag protein on CcdB killer activity.

#### **5.4 HT7 function in *P. falciparum***

*P. falciparum* transgenic parasites were establishing expressing *P. falciparum* dihydrofolate reductase thymidylate synthase (*Pf*DHFRTS) with a C-terminal HT7 tag. The DHFRTS-HT7 gene in transgenic parasites is under the control of a 5' HSP86 promoter. This is a strong constitutive promoter used to drive reporter gene expression in transgenic *P. falciparum* parasites (76). Transgenic parasites were *in vivo* labeled with TMR for DHFRTS-HT7 fusion protein localization (Shaw P.J., personal communication). Confocal microscopy was used for detecting the TMR signal in transgenic parasites. Although a TMR signal was observed in transgenic parasites, the signal was also present to a similar intensity in parental 3D7 non-transgenic parasite control strain. The signal remained in control cells, even after stringent washing to remove excess ligand from the cell. Therefore, this TMR signal could be noise since the TMR signal cannot be distinguished in transgenic from negative control parasite. Although it cannot be ruled out that DHFRTS-HT7 gene was not transcribed as mRNA (mRNA expression study was not performed), it appears that no DHFRTS-HT7 protein was made in transgenic parasites. To my knowledge, there is no report of similar problems of non-specific trapping of TMR ligand. The report by Camarda *et al.*, 2010 in which TMR labeling was used to detect a *Pf*g27-HT7 fusion protein showed expression in gametocytes as expected. Camarda *et al.*, 2010 used

HT7 protein for localization purpose only in the gametocyte stages of *P. falciparum*. Their data did not include any comparison of HT expression between blood and gametocyte stages, and data from control experiments of TMR labeling non-transgenic parasites, or any other suitable control cell were absent. Therefore, in *P. falciparum* blood stages, it is difficult to be certain if HaloTag fusion protein can be expressed properly. Lacking expression of *PfDHFRTS-HT7* in *P. falciparum* is consistent with the low activity of this protein in *E. coli* (see section 5.2). If more soluble and more stable HT variants could be found (see section 5.2), they could be of use in *Plasmodium falciparum*.

### 5.5 Fusion protein interference by HT7 for other proteins

Although HT7 is a more stable protein than HT2, and in general is expressed better as a fusion with other proteins (53), there are several reports in the literature of inactive HT7 protein fusions. Locatelli-Hoops *et al.*, 2012 demonstrated that a C-terminal HT7 lowered the expression of cannabinoid receptor protein CB2 fusion protein, but did not affect its functional activity in *E. coli*. In contrast, N-terminus tagged HT7-CB2 fusion protein was expressed at a higher level, but had low activity, presumably because of misfolding. In *E. coli*, N-terminal HT7 fusion tag was previously used to express 19 different fusion proteins (50). Although HT7 enhanced the expression of soluble target proteins, only two proteins were found to be active. In another report published by Motejaded *et al.* 2010, HT7 N-terminal tagged lipase was active when expressed in *E. coli*, but an additional N-terminal *maltE* (maltose binding protein) tag was needed for solubility. Recently, Chumanov *et al.*, 2011 published a report in which both N- and C- terminal HT7 tags were tolerated for the methyl transferase CRM1 protein when expressed in mammalian HEK293 cells. However in *E. coli*, the CRM1 fusion protein was highly insoluble when expressed with an N-terminal HT7 tag, whereas CRM1 activity was retained with a C-terminal HT7 tag (albeit to the cost of poor solubility and truncated forms of protein). Taken together, HT7 appears to be a poorly performing tag for fusion protein expression in *E. coli*, and perhaps other cells.



## 5.6 EGFP-HT2 function in *P. berghei*

*P. berghei* stable transgenic lines were generated expressing EGFP-HT<sup>WT</sup> and EGFP-HT2<sup>D106A</sup> fusion proteins in asexual stages. The transgenic line with EGFP-HT2<sup>D106A</sup> was used as a control for testing the specificity of haloalkane ligands directed against HT, since the mutant cannot form covalent complexes (see section 5.1). Transgenic parasites carrying EGFP-HT2 fusion genes integrated in the expected fashion at the *d-ribosomal-rrna* locus, as confirmed by PCR. The EGFP-HT2 genes in the transgenic parasites are expressed at the RNA level, as shown by RT-PCR. Due to lack of an appropriate control of transgenic parasites expressing EGFP only, it was not possible to quantify the actual expression of EGFP-HT<sup>WT</sup> and EGFP-HT<sup>D106A</sup> accurately. The EGFP-HT<sup>D106A</sup> protein expression was much weaker than EGFP-HT<sup>D106A</sup> in *E. coli* and *P. berghei* (unpublished observation) suggesting that HT may have a negative effect on overall protein stability in both cell types. It would be interesting to test whether the more stable HT7 variant also affects EGFP function/expression in *P. berghei*. It would also be interesting to compare the expression of N-terminus tagged with EGFP fusion protein to see affects the expression level. However, N-terminal HT7 may have a similar detrimental effect, since no transgenic parasite line was obtained expressing N-terminal Halo-tagged *Tg*-DHFRTS protein. It should be borne in mind though that the interpretation of interference of EGFP function/expression by HT2 in *P. berghei* must be tempered by the following caveats: a) comparison of the actual protein levels of EGFP-HT2 with *PbGFP* was not possible, since the former was not detectable by Western blot b) The levels of reporter RNA expression in EGFP-HT2 and *PbGFP* lines were not quantified c) The GFP variant expressed in *PbGFP* is different from that expressed in EGFP-HT2 lines (GFPmut3 and EGFP, respectively). Although the expression of EGFP-HT2 appears to be weak, it might be detected by Western blot if different protein extraction methods were used, or if another antibody against HT was used to immunoprecipitate and enrich for EGFP-HT2 first. To test whether EGFP-HT2 RNA was expressed at the same level as *PbGFP*, quantitative methods such as RT-qPCR, northern blot, or RNase protection assay could be performed. However, these methods would be difficult to implement because of the extensive sequence differences between EGFP and GFPmut3, i.e. design of probe capable of binding efficiently to both sequences is

difficult. Ideally, a control parasite line expressing EGFP alone would have been a more suitable control. However, EGFP appears to be at least as active as GFPmut3 in *P. berghei* and *P. falciparum* when expressed alone (80), or when fused to proteins other than HT2 (81, 82).

### 5.7 HT2 as a tool for controlling protein levels in *Plasmodium*

Overall, HT fusion proteins expression was low in *Plasmodium* species. The level of HT fusion protein appears to be lower when expressed in *Plasmodium* compared with mammalian cells; for example EGFP-HT2 was barely detectable when expressed in *P. berghei* (as shown by flow cytometry and fluorescence microscopy; data not shown), but was strongly expressed in mammalian cells (48, 55). The relatively higher expression of HT2 fusion proteins in mammalian cells means that the control of reporter protein with hydrophobic ligands can be accurately measured in these cells. HT2 mediated protein-controlling strategy requires the engagement of two important proteins from the cellular quality control network, namely HSP70 and CHIP or Parkin. Neklesa *et al.*, 2013 hypothesized that HT2 fusion protein bound to HyT13 hydrophobic ligand mimics an unfolded protein that is recognized by cytosolic HSP70 chaperone protein. This protein is the first step in UPR, during which protein refolding can occur. If the refolding process fails, or occurs too slowly, the unfolded protein is subsequently ubiquitinated either by CHIP or Parkin (83, 84) that subsequently engaged with HSP70 molecular chaperone. Ubiquitination of HT2 protein induced by the hydrophobic ligand complex engages the proteasome and fusion protein is ultimately destroyed. While it was not possible to assess whether the HT2 degron tool could be used in *Plasmodium* owing to low level of HT2 fusion protein expression, it is necessary to determine if *Plasmodium* parasites possess a UPR system that could mediate HT2 degron function. Bioinformatic genome analysis in PlasmoDB found that present in *P. berghei* and *P. falciparum* species possessed both HSP70 and CHIP homologues (**Table 4.1**). Even though quality control machineries necessary for HT2 protein degradation are present in *Plasmodium*, the low expression of HT2 fusions in *Plasmodium* would be a major obstacle since fusion protein levels would be low even in the absence of ligand.

**Table 5.1: UPR homologous proteins in *P. falciparum* (Pf) and *P. berghei* (Pb)**

<b>UPR protein involved in HaloTag degradation in mammalian cells</b>	<b>Homologs in <i>Pb</i></b>	<b>Homologs in <i>Pf</i></b>	<b>Annotated Protein Function</b>
Heat Shock Protein 70 (HSP70)	PF3D7_0818900	PBANKA_071190	Heat shock protein 70 (Hsp70)
C-terminus of Hsp70-interacting protein (CHIP)	PF3D7_0707700	PBANKA_080490	Ubiquitin-protein ligase E3

Although the essential elements of protein surveillance systems, including UPR are present in *Plasmodium*, they may function slightly differently from mammalian cells. deAzevedo *et al.* 2012 published a report describing that, different FKBP12 variants are stabilized less efficiently by Shield1 ligand in *P. falciparum* compared with mammalian cells. The trimethoprim-regulated ecDHFR degron is also less efficient in *P. falciparum* (37) compared with mammalian cells (85). Taken together, current inducible protein degradation tools are less powerful/not useful in *Plasmodium* compared with other cell types. Nonetheless, it could be interesting to test whether HT2-tagged proteins can be stabilized in *Plasmodium* using the recently described HT2 stabilizer HALTS (55).

## CHAPTER VI

### CONCLUSION

HaloTag function was tested in both *E. coli* and *Plasmodium*. Two different versions of HaloTag, namely HT2 and HT7 were used in this study. It was found that when fused to different proteins, both HT2 and HT7 led to markedly reduced protein levels. In cases where fusion protein expression could be detected, the fusion proteins had activity, albeit at low levels. A DHFRS-HT2 fusion protein was expressed at a lower level and had less activity than the corresponding HT7 fusion, similar to that reported for other proteins. The expression levels and activities of EGFP-HT2 proteins in *E. coli* and *P. berghei* were low. The lower expression of these proteins contrasts with the higher expression reported in mammalian cells. The low level of expression for different HaloTag fusion proteins in *Plasmodium* suggests that the use of this tool is limited in *Plasmodium* parasites

## REFERENCES

1. Hartl. (2004). The origin of malaria: mixed messages from genetic diversity. *Nat Rev Microbiol*, 2(1): 15-22.
2. The malERA Consultative Group on Drugs (2011). A Research Agenda for Malaria Eradication: Drugs. *PLoS Med.* 8(1): e1000402.
3. Gardner, M, J., Hall, N., Fung, E., & White, O. (2002). Genome sequence of the human malaria parasite *Plasmodium falciparum*. *Nature*. 419(6906): 498-511.
4. Carlton, J, M., Adams, J, H., & Silva, J.C. (2008). Comparative genomics of the neglected human malaria parasite *Plasmodium vivax*. *Nature*. 455(7214): 757-63.
5. Le Roch K.G., Zhou, Y., Blair, P, L., Grainger, M., Moch, J.K., & Haynes, J, D. (2003). Discovery of gene function by expression profiling of the malaria parasite life cycle. *Science*. 301 (5639): 1503–1508.
6. Bozdech, Z., Llinas, M., Pulliam, B.L., Wong, E.D., Zhu, J., & De, Risi., J.L. (2003). The transcriptome of the intraerythrocytic developmental cycle of *Plasmodium falciparum*. *PLoS Biol.* 1(1): e5.
7. Aurrecochea, C., Brestelli, J., Brunk, B, P., Dommer, J., Fischer, S., Gajria, B., et al. (2009) PlasmoDB: a functional genomic database for malaria parasites. *Nucleic Acids Res.* 37D, 539-43.
8. Wellems T, E., Walker-Jonah, A., & Panton, L.J.(1991). Genetic mapping of the chloroquine-resistance locus on *Plasmodium falciparum* chromosome 7. *Proc Natl Acad Sci U S A.* 88(8): 3382-6.
9. Sidhu, A, B., Verdier-Pinard, D., & Fidock, D. A. (2002) Chloroquine resistance in *Plasmodium falciparum* malaria parasites conferred by pfcrt mutations. *Science*. 298(5591): 210-3
10. Fonager, J., Franke-Fayard, B,M., Adams, J.H., Ramesar, J., Klop, O., & Khan, S, M. (2011). Development of the piggyBac transposable system for

- Plasmodium berghei* and its application for random mutagenesis in malaria parasites. *BMC Genomics*. 12:155.
11. Balu, B., Shoue, D.A., Fraser, M.J., Jr., & Adams, J.H. (2005). High-efficiency transformation of *Plasmodium falciparum* by the lepidopteran transposable element *piggyBac*. *Proc Natl Acad Sci USA*. 102 (45): 16391–16396.
  12. Maier, A.G., Rug, M., O'Neil, M.T., Brown, M., Chakravorty, S., & Szestak, T. (2008). Exported proteins required for virulence and rigidity of *Plasmodium falciparum* infected human erythrocytes. *Cell*. 134 (1): 48–61.
  13. Hammond, S. M. (2005). Dicing and splicing. The core machinery of the RNA interference pathway. *Febs Lett*. 579 (26): 5822–5829.
  14. McRobert, L., & McConkey, G.A. (2002). RNA interference (RNAi) inhibits growth of *Plasmodium falciparum*. *Mol. Biochem. Parasitol*. 119 (2): 273–278.
  15. Tuteja, R., Pradhan, A., & Sharma, S. (2008). *Plasmodium falciparum* signal peptidase is regulated by phosphorylation and required for intra-erythrocytic growth. *Mol. Biochem. Parasitol*. 157(2): 137–147.
  16. Kumar, R., Adams, B., Oldenburg, A., Musiyenko, A., & Barik, S. (2002). Characterization and expression of a PP1 serine/threonine protein phosphatase (PfPP1) from the malaria parasite, *Plasmodium falciparum*: demonstration of its essential role using RNA interference. *Malar. J*. 145, 1245–1254.
  17. Dasaradhi, P.V., Mohmmmed, A., Kumar, A., Hossain, M.J., Bhatnagar, R.K., Chauhan, V.S., and Malhotra, P. (2005). A role of falcipain-2, principal cysteine proteases of *Plasmodium falciparum* in merozoite egression. *Biochem. Biophys. Res. Commun*. 336 (4): 1062–1068.
  18. Mohmmmed, A., Dasaradhi, P.V., Bhatnagar, R.K., Chauhan, V.S., and Malhotra, P. (2003). In vivo gene silencing in *Plasmodium berghei*--a mouse malaria model. *Biochem. Biophys. Res. Commun*. 309 (3): 506–511.

19. Baum, J., Papenfuss, A.T., Mair, G.R., Janse, C.J., Vlachou, D., & Waters, A.P. (2009). Molecular genetics and comparative genomics reveal RNAi is not functional in malaria parasites. *Nucleic Acids Res.* 37(11): 3788-98
20. Lopez-Barragan, M, J., Lemieux, J., Quinones, M., Williamson, K, C., & Molina-Cruz A., (2011). Directional gene expression and antisense transcripts in sexual and asexual stages of *Plasmodium falciparum*. *BMC Genomics.* 12: 587.
21. Augagneur, Y., Wesolowski, D., Tae, H, S., Altman, S., & Ben Mamoun, C. (2012). Gene selective mRNA cleavage inhibits the development of *Plasmodium falciparum*. *Proc Natl Acad Sci U S A.* 109 (16): 6235–6240.
22. Lundblad, E, W., & Altman, S. (2010) Inhibition of gene expression by RNase P. *New Biotechnol.* 27 (3):212–221.
23. Meissner, M., Schüter, D., & Soldati, D. (2002). Role of *Toxoplasma gondii* myosin A in powering parasite gliding and host cell invasion. *Science.* 298 (5594): 837–840.
24. Gossen, M., & Bujard, H. (1992). Tight control of gene expression in mammalian cells by tetracycline-responsive promoters. *Proc Natl Acad Sci USA.* 89 (12):5547–5551.
25. Meissner, M., Brecht, S., Bujard, H., & Soldati, D. (2001). Modulation of myosin A expression by a newly established tetracycline repressor-based inducible system in *Toxoplasma gondii*. *Nucleic Acid Res.* 29 (22): E115.
26. Meissner, M., Krejany, E., Gilson, R.P., de Koning-Ward T.F., Soldati, D., & Crabb, B. S. (2005). Tetracycline analogue-regulated transgene expression in *Plasmodium falciparum* blood stages using *Toxoplasma gondii* transactivators. *Proc. Natl. Acad. Sci, USA.* 102 (8): 2980-5.
27. Duraisingh, T.M., Triglia, T., Ralph, A.S., Rayner, C.J., Barnwell, W.J., McFadden, I.G., & Cowman, F.A. (2003). Phenotypic variation of *Plasmodium falciparum* merozoite proteins directs receptor targeting for invasion of human erythrocytes. *The EMBO Journal.* 22 (5): 1047 – 1057.

28. Pino, P., Sebastian, S., Kim, E.A., Bush, E., Brochet, M., & Volkmann, K. (2012). A Tetracycline-Repressible Transactivator System to Study Essential Genes in Malaria Parasites. *Cell Host Microbe*. 12(6): 824-34.
29. Watson, P, Y., & Fedor, M.J. (2011). The glmS riboswitch integrates signals from activating and inhibitory metabolites in vivo. *Nat Struct Mol Biol*. 18 (3): 359–363.
30. Prommana P, Uthaipibull C, Wongsombat C, Kamchonwongpaisan S, Yuthavong Y, et al. (2013). Inducible Knockdown of *Plasmodium* Gene Expression Using the glmS Ribozyme. *PLoS ONE*. 8(8): e73783.
31. Sleeb, B, E., Lopaticki, S., & Marapana, D.S. et al. (2014). Inhibition of Plasmeprin V Activity Demonstrates Its Essential Role in Protein Export, PfEMP1 Display, and Survival of Malaria Parasites. *PLoS Biol*. 12(7): e1001897.
32. Varshavsky, A. (1992). The N-end rule. *Cell* 69. 725–735.
33. Park, E.C., Finley, D., & Szostak, J.W. (1992) A strategy for the generation of conditional mutations by protein destabilization. *Proc. Natl. Acad. Sci. USA*. 89 (4): 1249– 1252.
34. Smith, M, H., Ploegh, H. L., & Weissman, J.S. (2011) Road to ruin: targeting proteins for degradation in the endoplasmic reticulum. *Science*. 25; 334(6059): 1086.
35. Banaszynski, L.A., Chen, L.C., Maynard-Smith, L.A., Ooi, A.G., and Wandless, T.J. (2006). A rapid, reversible, and tunable method to regulate protein function in living cells using synthetic small molecules. *Cell*. 126(5): 995–1004.
36. Armstrong, C.M., & Goldberg, D.E. (2007). An FKBP destabilization domain modulates protein levels in *Plasmodium falciparum*. *Nat Methods*. 4 (12): 1007-9.
37. Muralidharan, V., Oksman, A., Iwamoto, M., Wandless, J.T., & Goldberg, E.D. (2011). Asparagine repeat function in a *Plasmodium falciparum* protein assessed via a regulatable fluorescent affinity tag. *Proc. Natl. Acad. Sci, USA*. 108(11): 4411–4416.



38. Russo, I., Oksman, A., Vaupel, B., & Goldberg, D.E. (2009) A calpain unique to alveolates is essential in *Plasmodium falciparum* and its knockdown reveals an involvement in pre-S-phase development. *Proc. Natl. Acad. Sci USA*. 106 (5): 1554-9.
39. Dvorin, J.D., Martyn, D.C., Patel, S.D., Grimley, J.S., Collins, C.R., Hopp, C.S., et al. (2010). A plant-like kinase in *Plasmodium falciparum* regulates parasite egress from erythrocytes. *Science*. 328(5980): 910-2.
40. de Azevedo, M, F., Gilson, P, R., Gabriel, H, B., Simões, R, F., Angrisano, F., et al. (2012) Systematic Analysis of FKBP Inducible Degradation Domain Tagging Strategies for the Human Malaria Parasite *Plasmodium falciparum*. PLoS ONE 7(7): e40981.
41. Bongor, K.M., Chen, L.C., Liu, C.W., and Wandless, T.J. (2012) Small-molecule displacement of a cryptic degron causes conditional protein degradation. *Nat. Chem. Biol.* 7(8): 531-7.
42. Lins, L., & Brasseur, R., Te. (1995) Hydrophobic effect in protein folding. *FASEB J.* 9, 535–540.
43. Kubota, H. (2009). Quality control against misfolded proteins in the cytosol: a network for cell survival. *J. Biochem.* 146(5): 609–616.
44. Malhotra, J, D., & Kaufman, R. J. (2007). The endoplasmic reticulum and the unfolded protein response. *Semin Cell Dev Biol.* 18(6): 716–731.
45. Vembar, S. S., & Brodsky, J. L. (2008). One step at a time: endoplasmic reticulum associated degradation. *Nat. Rev. Mol. Cell Biol.* 9(12): 944–957.
46. Hetz, C. (2012). The unfolded protein response: controlling cell fate decisions under ER stress and beyond. *Nat. Rev. Mol. Cell Biol.* 13(2), pp.89–102.
47. Nair, U., & Klionsky, D. J. (2005). Molecular mechanisms and regulation of specific and nonspecific autophagy pathways in yeast. *J. Biol. Chem.* 280(51): 41785–41788.
48. Neklesa, T, K., Tae, H, S., Schneekloth, A, R., Stulberg, M, J., Corson, T, W., & Sundberg, T, B. (2011). Small-molecule hydrophobic tagging-induced degradation of HaloTag fusion proteins. *Nat. Chem. Biol.* 7(8): 538-43.

49. Janssen, D.B. (2004). Evolving haloalkane dehalogenases. *Curr Opin Chem Biol.* 8(2): 150- 9.
50. Ohana, R, F., Encell, L, P., Zhao, K. et al., (2009). HaloTag7: a genetically engineered tag that enhances bacterial expression of soluble proteins and improves protein purification. *Protein Expr Purif.* 68(1): 110-20.
51. Los, G, V., and Wood, K. (2007). The HaloTag: A novel technology for cell imaging and protein analysis. *Methods Mol Biol.* 356: 195-208.
52. Los, V.G., Encell, P.L. McDougall et al., 2008. HaloTag: A Novel Protein Labeling Technology for Cell Imaging and Protein Analysis. *ACS Chem. Bio.* 3(6): 373–382.
53. Encell, L, P., Friedman, O, R., Zimmerman K. et al., 2012. Development of a dehalogenase-based protein fusion tag capable of rapid, selective and covalent attachment to customizable ligands. *Curr Chem Genom.* 6:55-71.
54. Urh M., & Rosenberg M. (2012). HaloTag, a Platform Technology for Protein Analysis. *Curr Chem Genomics*, 6:72-8.
55. Neklesa, T, K., Noblin, D,J., Kuzin, A., Lew, S., Seetharaman, J., & Acton, T. B. (2013). A bidirectional system for the dynamic small molecule control of intracellular fusion proteins. *ACS Chem Biol.* 8(10): 2293-300.
56. Camarda, G., Bertuccini, L., Singh, S.K., Salzano, A.M., Lanfrancotti, A., & Olivieri, A. (2010). Regulated oligomerisation and molecular interactions of the early gametocyte protein Pfg27 in *Plasmodium falciparum* sexual differentiation. *Int. J Parasitol.* 40(6): 663-73.
57. Luxananil, P., Promchai, R., Wanasen, S. et al., 2009. Monitoring *Lactobacillus plantarum* BCC 9546 starter culture during fermentation of Nham, a traditional Thai pork sausage. *Int J Food Microbiol.* 129(3): 312-5.
58. Franke-Fayard, B., Trueman, H., Ramesar, J., Mendoza, J., van der Keur, M., & van der Linden, R. (2004). A *Plasmodium berghei* reference line that constitutively expresses GFP at a high level throughout the complete life cycle. *Mol Biochem Parasitol.* 137(1): 23-33.

59. van Spaendonk, R, M, L., Ramesar, J., & van Wigcheren, A. (2001). Functional equivalence of structurally distinct ribosomes in the malaria parasite *Plasmodium berghei*. *J Biol Chem.* 276(25): 22638–47.
60. Tae, S, H., Roth, G, A., Sundberg, B, T., Raina, K., Neklesa, K.T., & Crews, M, C (2012). Identification of Hydrophobic Tags for the Degradation of Stabilized Proteins. *Chem. Bio. Chem.* 13 (4): 538-541.
61. Rath, A., Glibowicka, M., Nadeau, V.G., Chen, G., & Deber, C.M. (2009). Detergent binding explains anomalous SDS-PAGE migration of membrane proteins. *Proc Natl Acad Sci U S A.* 106 (6): 1760-5.
62. Chitnumsub, P., Yuvaniyama, J., Vanichtanankul, J., Kamchonwongpaisan, S., Walkinshaw, M, D., & Yuthavong, Y. (2004). Characterization, crystallization and preliminary X-ray analysis of bifunctional dihydrofolate reductase-thymidylate synthase from *Plasmodium falciparum*. *Acta Crystallogr D Biol Crystallogr.* 60 (4): 780-3.
63. Kamchongwongpaisan, S., Suwanakitty, N., & Yuthavong, Y. (2012). A bacterial surrogate for testing of antimalarials: thyA knockout and folA knockout bacteria for testing of inhibition of malarial dihydropfolate reductase-thymidylate synthase. WO2012108845.
64. Bernard, P., & Couturier, M. (1992). Cell killing by the F plasmid CcdB protein involves poisoning of DNA-topoisomerase II complexes. *Mol. Biol.* 226(3): 735–745.
65. Baker, T, A., & Sauer, R.T. (2012). ClpXP, an ATP-powered unfolding and protein-degradation machine. *Biochim Biophys Acta.* 1823(1):15–28.
66. Guan, L., Liu, Q., Li, C., & Zhang, Y. (2013). Development of a Fur-dependent and tightly regulated expression system in *Escherichia coli* for toxic protein synthesis. *BMC Biotechnology.* 13:25.
67. Bernard, P., K. Kézdy, L., Van Melderren, J., Steyaert, L., Wyns, M, L., & Pato, N.P. (1993). The F plasmid CcdB protein induces efficient ATP-dependent DNA cleavage by gyrase. *J. Mol. Biol.* 234 (3): 534-541.
68. Bex, F., Karoui, H., Rokeach, L., Dreze, P., Garcia, L., & Couturier, M. (1983). Mini-F encoded proteins: identification of a new 10.5 kilodalton species. *EMBO J.* 2(11): 1853–1861.

69. Bernard, P. (1996). Positive Selection of Recombinant DNA by CcdB *Biotechniques*. 21(2): 320-3.
70. Tseng, J, C., Benink, H,A., McDougall, M,G., Chico-Calero, I., & Kung, A. L. (2012) In Vivo Fluorescent Labeling of Tumor Cells with the HaloTag® Technology. *Curr Chem Genomics*. 6:48-54.
71. Friedman, O, R., Encell, L, P. & Zhao, K. et al. 2009. Halo Tag7: a genetically engineered Tag that enhances bacterial expression of soluble proteins and improves protein purification. *Protein Expr. Purif*. 68 (1): 110-20.
72. Peterson, S, N., & Kwon, K. (2012). Application of a novel HaloTag to characterize protein-protein and protein-DNA interactions. *Curr Chem Genom*, 6: 8-17.
73. Singh, V., Wang, S., & Kool, E.T. (2013). Genetically encoded multispectral labeling of proteins with polyfluorophores on a DNA backbone. *J Am Chem Soc*.135(16): 6184-91.
74. Bahassi, E, M., Salmon, M, A., Van Melderren, L., Bernard, P., & Couturier, M. F. (1995). Plasmid CcdB killer protein: ccdB gene mutants coding for non-cytotoxic proteins which retain their regulatory functions. *Mol Microbiol*. 15(6): 1031-7.
75. Dao-Thi, M, H., Van Melderren, L., De Genst, E., Afif, H., Buts, L., Wyns, L., & Loris, R. (2005). Molecular basis of gyrase poisoning by the addiction toxin CcdB. *J Mol Biol*. 348(5): 1091-102.
76. Wu, Y., Sifri, C. D., Lei, H, H., Su, X, Z., & Wellems, T. E. (1995) Transfection of *Plasmodium falciparum* within human red blood cells. *Proc. Natl. Acad. Sci. USA* 92, 973–977.
77. Locatelli-Hoops, S., Sheen, F,C., Zoubak, L., Gawrisch, K., & Yeliseev, A. A. (2013). Application of HaloTag technology to expression and purification of cannabinoid receptor CB2. *Protein Expr Purif*. 89(1): 62-72.
78. Motejadded, H., Kranz, B., Berensmeier, S., Franzreb, M., & Altenbuchner, J. (2010). Expression, one-step purification, and immobilization of HaloTag<sup>(TM)</sup> fusion proteins on chloroalkane-functionalized magnetic beads. *Appl Biochem Biotechnol*.162 (7): 2098-110.

79. Chumanov, R, S., Kuhn, P,A., Xu, W., & Burgess, R.R. (2011). Expression and purification of full-length mouse CARM1 from transiently transfected HEK293T cells using HaloTag technology. *Protein Expr Purif.* 76(2): 145-53.
80. Straimer, J., Lee, M,C. and Lee, A.H. et al., (2012). Site-Specific Editing of the *Plasmodium falciparum* Genome Using Engineered Zinc-Finger Nucleases. *Nat Methods.* 9(10): 993-8.
81. Saeed, S., Carter, V., Tremp, A,Z., & Dessens, J.T. (2013) Translational repression controls temporal expression of the *Plasmodium berghei* LCCL protein complex. *Mol Biochem Parasitol.*189 (1-2): 38-42.
82. Carter, V., Shimizu, S., Arai, M., & Dessens, J.T.(2008). PbSR is synthesized in macrogametocytes and involved in formation of the malaria crystalloids. *Mol Microbiol.* 68(6): 1560-9.
83. Petrucelli, L., Dickson, D., & Kehoe, K. (2004). CHIP and Hsp70 regulate tau ubiquitination, degradation and aggregation. *Hum Mol Genet.* (2004) 13(7): 703-14.
84. Moore, D, J., West, A, B., Dikeman, D,A., Dawson, V. L., & Dawson, T. M. (2008) Parkin mediates the degradation-independent ubiquitination of Hsp70. *J Neurochem.* 105(5): 1806-19.
85. Iwamoto, M., Björklund, T., Lundberg, C., Kirik, D., & Wandless, T.J.(2010) A general chemical method to regulate protein stability in the mammalian central nervous system. *Chem Biol.* 17(9): 981-8.
86. Fidock, D.A., & Wellems, T.E. (1997) Transformation with human dihydrofolate reductase renders malaria parasites insensitive to WR99210 but does not affect the intrinsic activity of proguanil. *Proc. Natl. Acad. Sci. USA,* 94(20): 10931-10936.
87. Hillcoat, B, L., Nixon, P, F., & Blakley, R. L. (1967). Effect of substrate decomposition on the spectrophotometric assay of dihydrofolate reductase. *Analytical biochemistry.* 21(2): 178-89.
88. Wang, W., & Malcolm, B.A. (1999). Two-stage PCR protocol allowing introduction of multiple mutations, deletions and insertions using QuikChange site-directed mutagenesis. *BioTechniques.* 26(4): 680-682.

89. Witte, A., Wanner, G., Sulzner, M., & Lubitz, W. (1992). Dynamics of PhiX174 protein E-mediated lysis of *Escherichia coli*. *Arch Microbiol.* 13(4): 381–388.
90. Bradford, M. M. (1976). A rapid and sensitive method for the quantitation of microgram quantities of protein utilizing the principle of protein-dye binding. *Anal Biochem.* 72: 248-54.
91. Quan, J, & Tian, J. (2009). Circular Polymerase Extension Cloning of Complex Gene Libraries and Pathways. *PLoS ONE*, 4(7): e6441.
92. Trager, W, & Jensen, J. B. (1976). Human malaria parasites in continuous culture. *Science* 193(4254): 673-5.
93. Lambros, C, & Vanderberg, J. P. (1979). Synchronisation of *Plasmodium falciparum* erythrocytic stages in culture. *Journal of Parasitology*, 65(3): 418-20.
94. Feliciello, I, & Chinali, G. (1993). A modified alkaline lysis method for the preparation of highly purified plasmid DNA from *Escherichia coli*. *Anal Biochem.* 212(2): 394-401.
95. Crabb, B, S., Rug, M., Gilberger, T, W., Thompson, J, K., Triglia, T., Maier, A, G, & Cowman, A. F. (2004). Transfection of the human malaria parasite *Plasmodium falciparum*. *Methods Mol Biol.* 270:263-76.
96. Janse, C, J., Franke-Fayard, B., Mair, G, R., Ramesar, J., Thiel, C, & Engelmann, S. et al. (2006). High efficiency transfection of *Plasmodium berghei* facilitates novel selection procedures. *Mol Biochem Parasitol.* 145(1): 60-70.
97. Halbert, J., Ayong, L., Equinet, L., Roch, K.L., Hardy, M.G., & Dean, R.L. et al. (2010). A *Plasmodium falciparum* Transcriptional Cyclin-Dependent Kinase-Related Kinase with a Crucial Role in Parasite Proliferation Associates with Histone Deacetylase Activity. *Eukaryotic cell*, 9 (6): 952–959.

## **BIOGRAPHY**

<b>NAME</b>	Md. Golam Rizvee Ahmed
<b>DATE OF BIRTH</b>	1 <sup>st</sup> December 1988
<b>PLACE OF BIRTH</b>	Chandpur, Bangladesh
<b>INSTITUTION ATTENDED</b>	Assumption University, 2006-2010 Bachelor of Science, (Agro-Industry) Mahidol University, 2011-2014 Master of Science, (Biochemistry)
<b>SCHOLARSHIP RECEIVED</b>	Department of Biochemistry, Faculty of Science, Mahidol University
<b>HOME ADDRESS</b>	Village: Nayani-Lakshmipur, P.O. West- Charkrisnapur, Road / Thana : Haimchar, District: Chandpur.
<b>PRESENTATION</b>	Joint International Tropical Medicine Meeting (JITMM) conference, Bangkok, Thailand.